Fall 2023

Renewable Fuels: Molecular Dynamics Investigations Into Pyrolysis of Methyl Linoleate

Elson Osakpolor Eguaosa
Missouri State University, eoe89s@MissouriState.edu

ENGINEERING VIABLE RENEWABLE FUELS: MOLECULAR DYNAMICS INVESTIGATIONS INTO PYROLYSIS OF METHYL LINOLEATE

A Master's Thesis

Presented to

The Graduate College of

Missouri State University

In Partial Fulfillment

Of the Requirements for the Degree

Master of Science, Chemistry

By

Elson Osakpolor Eguaosa

December 2023

ENGINEERING VIABLE RENEWABLE FUELS: MOLECULAR DYNAMICS INVESTIGATIONS INTO PYROLYSIS OF METHYL LINOLEATE

Chemistry and Biochemistry

Missouri State University, December 2023

Master of Science

Elson Osakpolor Eguaosa

ABSTRACT

With the rapid depletion of the world's supply of fossil fuels, especially petroleum products, petroleum prices have risen by approximately 800% between the 1970s and now and are projected to continue rising. It is also expected that the world's consumption of energy will increase commensurate with its growing population. Although biodiesel is a good renewable alternative, it has its limitations including high production costs and poor low-temperature performance. We seek to improve conventional biodiesel with pyrolysis to produce low molecular-weight compounds with high energy densities. Understanding the pyrolysis path on the atomic scale is key as it will allow us to determine and engineer adequate reactants that maximize yield of desired energy producing molecules. An in-house generated database of 100 *ab initio* trajectories of methyl linoleate were examined for significant bond-breaking and bond-forming events. The times of the events and the position in the molecule were logged. These are tested against an in-house computer-automated analysis method, and comparison of the results will be presented. Quantum chemical techniques were also used to compute thermodynamic properties of the resulting fragments.

KEYWORDS: biodiesel, fatty-acid methyl esters, methyl linoleate, molecular dynamics, pyrolysis

ENGINEERING VIABLE RENEWABLE FUELS: MOLECULAR DYNAMICS INVESTIGATIONS INTO PYROLYSIS OF METHYL LINOLEATE

By

Elson Osakpolor Eguaosa

A Master's Thesis
Submitted to the Graduate College
Of Missouri State University
In Partial Fulfillment of the Requirements
For the Degree of Master of Science, Chemistry

December 2023

Approved:

Matthew R. Siebert, Ph.D., Thesis Committee Chair

Cyren Rico, Ph.D., Committee Member

Gautam Bhattacharyya, Ph.D., Committee Member

Siming Liu, Ph.D., Committee Member

Julie Masterson, Ph.D., Dean of the Graduate College

ACKNOWLEDGEMENTS

I would like to express my deepest gratitude and appreciation to my advisor, Dr. Siebert, for his invaluable guidance, support, and mentorship throughout my research journey. Their expertise, encouragement, and unwavering commitment to my academic and personal growth have been instrumental in shaping the outcome of this work.

I would also like to extend a heartfelt acknowledgment to my family, particularly my mother. Their constant love, understanding, and encouragement have been my anchor and source of strength during this challenging endeavor. Their unwavering belief in my abilities and their continuous support have been the driving force behind my achievements.

I dedicate this thesis to my late dad, Rest Osahon Eguaosa, whose presence in my life was brief but impactful. Though our time together was limited, I am grateful for the godly values he instilled in me, which have shaped the person I am today. His influence continues to guide me, and I carry his memory with me as a source of inspiration and strength.

TABLE OF CONTENTS

LIST OF TABLES

LIST OF FIGURES

CHAPTER 1: INTRODUCTION

1.1 Petroleum and its Applications

Petroleum, although naturally occurring, is a non-renewable resource. It is non-renewable because of the way it is formed. It is formed from biological deposits, dating back to millions of years, that has gone through pressure and temperature from layers of silt and sand that covered them over time.[1,2] It has been widely used in many areas of human endeavor. Petroleum has been used for energy production: for heating and powering electrical appliances; for production of fuels like gasoline, kerosene and diesel; for synthesis of organic compounds; for production of other petrochemical products like petroleum jelly, lubricants and tar; and polymers.[1,2] Petroleum is made up of parafins, naphthenes, olefins, aromatics and asphaltics,[3,4] all of which are very useful as precursors of products with very wide range of application. For instance, approximately 85% of a typical barrel of crude oil is used in the production of fuels for mobility and power generation, while the other 15% is converted into more than a dozen other petroleum products.[5] Parafins are used to produce most liquid fuels. In fact, 80% Naphthenes, which are cyclic saturated hydrocarbons, are used as solvents and fuel precussors.[6] Olefins are predominantly used for production of polymers, which are materials for manufacturing plastics.[7,8] Aromatics have been found to have many applications in organic chemistry, especially as solvent in both consumer and industrial products and as gasoline additives.[9] Asphaltics are used extensively in building and construction.[10] Figure 1 is a graphic representation of the distribution of petrochemical applications. Just like many other resources come with limitations and problems, petroleum has its problems. Complications of petroleum is discussed later in this chapter, but one

of such is the environmental pollution caused by combustion of petroleum products for energy purposes.

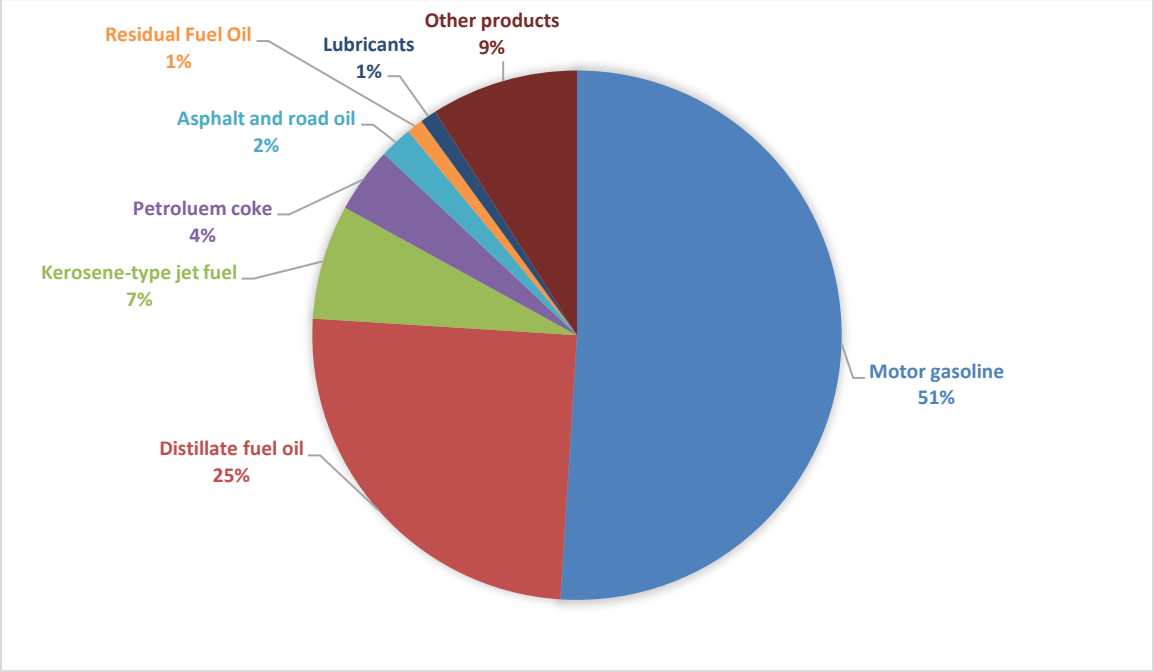

Figure 1. Applications of petroleum.[11]

Although petroleum has adverse environmental effects, it is still very useful and would be very difficult to do away with. However, humans must prepare for such a time when there would be no choice but actually stop using petroleum because it would just not be available, being a non-renewable resource.[2,12] Bearing this in mind, it is only natural to begin to look for alternatives for petroleum, and certain criteria, will play significant roles in determining best alternatives.

1.2 Problems with Petroleum

As earlier mentioned, petroleum requires millions of years to form.[2] This translates to a very high consumption to formation ratio which will lead to exhaustion. It has been estimated that crude oil reserves have about 54 years left for total consumption globally.[12] Fossil fuels

account for 80-83% of energy consumption, with petroleum contributing 31%.[2,13] Energy has tremendous effects on several areas of human endeavor, making the finite nature of petroleum very upsetting and it calls for very urgent attention. As we approach the extinction of petroleum, it is expected that prices will increase due to higher demand for the limited resource. Higher prices will lead to economic recessions and international conflicts, especially for some developing countries.[2] In finding an alternative, sustainability sets a foundation as to what should be sought, but other complications with petroleum raises concerns that should be considered.

Another major problem with petroleum is its negative impact on the environment. When fossil fuels, petroleum included, are extracted, refined, or burned for energy production, some toxic gasses are emitted, including carbon oxides (CO, CO_2), nitrogen oxides (NO_x), sulfur dioxide (SO_2), and hydrocarbons (e.g. CH_4).[2,14] These toxic emissions contribute to several harmful effects on humans and animals, including heart disorders, eye irritation, respiratory issues, and problems with the central nervous system.[14] Also, fine particulate matters are emitted from petroleum combustion and have been linked to increases in various diseases.[15] The emission of CO_2 is of particular interest as it is a primary driver of the greenhouse effect, and consequently climate change.[14,16–18] CO_2 emissions account for 80% of the contribution made by greenhouse gases to global warming.[19,20] The greenhouse effect happens when certain greenhouse gases (GHG) in the Earth's atmosphere trap heat and warm the planet's surface by retaining some of the reflected energy from the sun.[17,18] Although this process is important for life on Earth (it keeps the planet warm enough to support most forms of life), burning fossil fuels results in the emission of greenhouse gases and increases their concentrations in the environment. This results in an enhanced greenhouse effect and consequently global warming. As a result of combustion of fuels, CO_2 levels are climbing, leading to acid rains. Equations 1

and 2 represents the chemical conversion of fuels to CO_2 and CO_2 as a precursor of acid rain. Acid rain results in structural degradations and many other negative effects on various ecosystems including aquatic (threatening the life of fishes and amphibians) and terrestrial (leaching away minerals and nutrients for plants) habitats.[14,16,21]

$$C_xH_y + O_2 \rightarrow CO_2 + H_2O \quad (1)$$

$$CO_2 + 2\,H_2O \leftrightarrow HCO_3^- + H_3O^+ \leftrightarrow H_2CO_3 + H_2O \quad (2)$$

Equation 1 & 2. Chemical equations representing combustion of hydrocarbons (a major component of fossil fuels) resulting in the formation of CO2 and CO2 as a precursor for acid rain.[22]

Another environmental concern is spillage of petroleum during extraction, refining, and distribution. While oil spills happen most in marine environments, oil or petroleum products may be spilled from rig, tankers and other offshore facilities causing harmful environmental effects on other ecosystems.[23,24] The spills are also costly due to loss of the valuable resource and cost of cleaning up the spills.[23] Several technologies like CO_2 capture and sequestration and modification of automobile engines (use of catalytic converters, as well as redesign of engines to burn less fuel) have been employed to reduce emission of greenhouse gases.[19] Considering the risks to the environment and the health of the public, regulatory bodies have put strict standards on petroleum operations.[24,25] These standards have led to the development of technologies to mitigate risks at extraction and processing levels, which have also led to high costs of processing. Also, countries experience international pressure because of the global warming issues caused by petroleum operations.[2] Many deadly international wars have also been linked to petroleum operations.[26] These wars would lead to other problems like loss of livelihoods and economic instability.[27] As Russia is a big oil producer, the Russia-Ukraine war has had negative effects on economies that are dependent on oil imports from Russia.[27–29] The US and other

western countries placed a ban on Russian oil import as an economic sanction, and this has led to high pump prices, increased electricity bills and consequently inflation.[27,28]

In its entirety, petroleum is problematic is many ways and by understanding the problematic sides of petroleum use, the factors in Table 1 should be considered when choosing a suitable alternative.

Table 1. Factors to consider when choosing a suitable alternative for petroleum.

Factor	Description	Reason
Renewable	Alternative should be produced at a higher rate than it is consumed	Remove the risk of getting exhausted.
Environmentally benign	Operations with the alternative should not have negative effects on the environment, specifically reduced CO_2 emissions	Preserve the environment, reduce environmental problems like climate change and increase biodiversity.
Relatively local	Source for alternative should be relatively domestic.	Mitigate international pressures, wars, and economic instability.
Multipurpose	Alternative should be useful for energy, as well as other day to day purposes.	Effectively replace petroleum as a precursor for several applications like construction, cleaning, polymer processing.

1.3 Alternatives to Petroleum

Although petroleum has all the problems explained in the previous section, mankind has found ways to reduce the impacts of these problems. However, if we do get to a point where all global oil wells are exhausted, petroleum would just not be available for use. Thus, it is important to emphasize that renewability forms the foundation of our search for alternatives. Furthermore, energy is very useful in modern day and 80% of energy consumption comes from fossil fuels, with petroleum accounting for about 31%.[2,13] What this points to is that energy

would be the major problem to deal with in the event of an exhaustion. In light of this, renewable energy sources will be presented and examined for alignment with the other three criteria in Table 1.

Wind energy has been in use for over two thousand years and is viewed as a good source of clean energy.[30] With lots of research and development in wind energy, costs of generating electricity from wind has fallen by over 80%.[30] However, this potential alternative is known to be responsible for deaths of birds and bats, and a direct cause of noise pollution. [30,31] Electricity generation from wind has also impacted land surface atmosphere as energy, mass and moisture are exchanged between lower and upper-level air, leading to significant warming in wind-farm regions.[31] As is also expected, local climate influences the speed and availability of wind. Furthermore, while wind seems to be a greener alternative for energy production than petroleum is, it lacks that multipurpose capability and cannot be used for the many other things that petroleum can be used for. Therefore, wind would not be a suitable replacement for petroleum on the basis of relative locality and multi purposefulness.

Solar photovoltaic (PV) modules have been used to generate electricity from sunlight for about 150 years, and just like wind power generation, the PV system cost and performance have improved.[30] However, solar PV modules would still not be a suitable alternative for petroleum as it largely dependent on local climate as little or no energy can be generated during the night or winter seasons.[32] Solar PV modules lack the multi purposefulness that petroleum has, this also eliminates it as a suitable replacement.

Hydroelectric power is the largest and most efficient renewable resource used for generating electricity.[30] About 19% of global electricity production comes from hydropower.[30] The energy of the gravitational force of falling or flowing water is exploited to generate

electricity.[33] Although it has been reported that hydroelectric power has a considerable lower emission of CO_2, large dams do not reduce emissions of total greenhouse gases, such as CO_2 and CH_4, when compared with a fossil fuel power plant.[30,33,34] CO_2 emissions result from the decomposition of the exposed parts of trees that remain upright in the reservoir, while methane emissions originate from the decay of soft vegetation in anaerobic conditions at the bottom of the reservoir.[34] As an example, it has been reported that the Curu´a-Una Dam in the Amazonian portion of Brazil released 3.6 times the amount of greenhouse gases that would have been generated if the same amount of electricity had been produced from oil in 1990 (13 years after it has been filled).[34] There are other environmental concerns like reduction in biodiversity in aquatic ecosystems, poor water quality, spread of water related diseases, as well as flooding and consequent displacement of people.[30,33] Also, as climate also affect rainfall and level of water bodies, hydroelectricity generation is dependent on the local climate of a region. With all of these, it can be concluded that hydropower will not be a suitable replacement for petroleum as it doesn't meet any of the other three criteria.

Geothermal energy is a renewable energy source where energy is obtained from heat in the earth. The heat has been used commercially to generate electricity, and even directly, for about 70 years. Geothermal energy is a huge energy resource, and it is estimated that the uppermost 10 kilometers of the Earth's crust holds energy that is approximately 500 times greater than the energy available in all the earth's oil and gas reserves. Although this makes it a viable energy source, it is typically not evenly distributed, and it is often too deep to be exploited efficiently and economically due to its lack of concentration.[30] There are also environmental concerns with this renewable energy source. Geothermal fluids from plant operations constitutes a potential source of chemical pollution because they contain gases such as CO_2, hydrogen

sulfide (H_2S), ammonia (NH_3), mercury, radon, arsenic and boron.[30,35] Other forms of pollution that arises from the use of geothermal energy include thermal pollution and noise pollution. With all of these problems associated with geothermal energy, it will not be a suitable replacement for petroleum, as it does not meet the relative locality and multi purposefulness criteria.

Biomass energy refers to energy harvested from any organic matter derived from living or recently living organisms. Plants need energy for their growth and have a system of storing energy from sunlight called photosynthesis. Biomass was the earliest source of energy harnessed by man. Wood has always been burnt to generate heat, but modern technologies have emerged and have been used to convert biomass into more convenient forms like gases, liquids and electricity for both residential and industrial uses. Since plants exist in different forms, all year round, globally, it is safe to say that biomass meets the relative locality criterion. Biomass is also multifunctional as it has been used for producing materials such as paper, wood for construction and cotton for clothes. For the alternative to be considered environmentally benign, it should have significant reduction of GHG emissions, particularly CO_2. Although, combustion of biomass still releases significant levels of CO_2 to the environment, it is not considered as a contributor to climate change because plants used for biomass energy absorb carbon dioxide during photosynthesis when growing and release it back into the atmosphere when used for energy, resulting in no net increase in atmospheric carbon levels.[36,37] Biomass meets all criteria and would represent a suitable replacement for petroleum. Figure 2 is a graphic representation of analysis of renewable energy sources that have been discussed.

Biomass, as mentioned before, is a term used for all organic material gotten from plants and animals. As such, biomass is classified into subgroups namely: woody biomass which

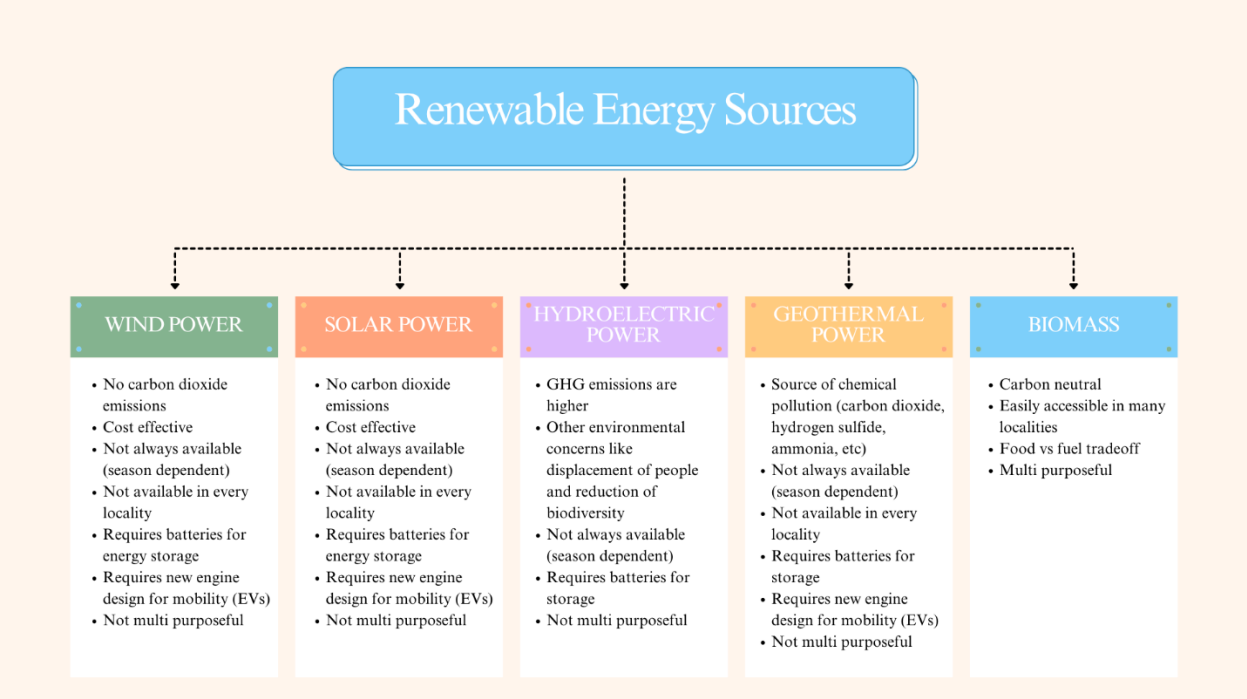

Figure 2. Illustrative analysis of renewable energy sources with pros and cons.[30–37]

generally consists of trees and root residues; herbaceous biomass which are from plants that have non-woody stem; aquatic biomass is obtained from aquatic ecosystems including algae and emerging plant; animal and human waste biomass; and biomass mixtures usually obtained from landfills.[30,38]Although biomass has always been in use, with more development, biomass has several benefits such as reducing greenhouse gas emissions, providing energy security, creating jobs in rural areas, and reducing dependence on fossil fuels.[30,38] Figure 3 gives a graphic illustration of the uses of biomass, including energy production.

However, biomass needs to go through several conversion technologies to produce other energy products including electricity, heat, liquid biofuels such as bioethanol and biodiesel, and biogas. Liquid biofuels are potential alternatives for liquid fuels obtained from petroleum used in the transport sector and have witnessed high production growth over the years. [36,38] They are gotten from energy crops, which is one of the main groups of herbaceous biomass.[38] These

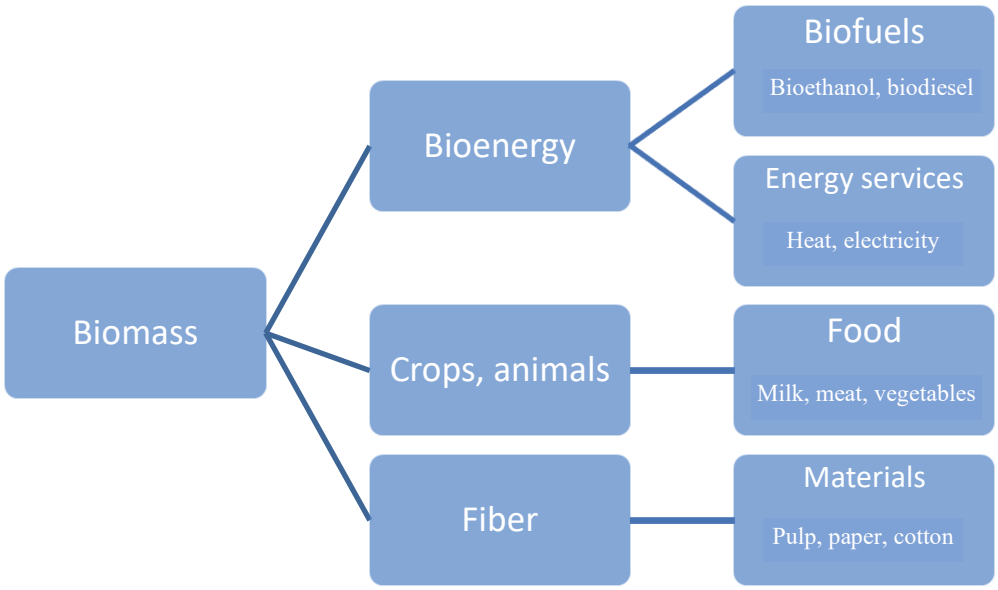

Figure 3. An illustration of the multi purposefulness of biomass.[30]

energy crops are converted to energy carriers via a variety of technologies. These technologies are largely thermo-chemical, biochemical or physico-chemical conversion processes.[38] Biodiesel is of particular interest because it has been used to replace small amounts of diesel. However, biodiesel can only be produced from oil producing plants such as soybeans and rapeseed that can produce compounds similar to hydrocarbons in petroleum.[30] This leads to the tradeoff of food for fuel, a common setback for the use of biomass because some plants used for biomass energy are essentially food crops. Although the multi purposefulness of biomass have been illustrated in Figure 3, another reason why biodiesel is of great interest is that it can be explored specifically for other applications that are peculiar to petroleum. This is possible via a thermochemical conversion technology called pyrolysis.

1.4 A Promising Alternative: Biodiesel

Biodiesel is a renewable and sustainable alternative fuel that is made from vegetable oils or animal fats.[39,40] It is a subclass of biofuel that has been used in diesel engines without any

modifications. Biodiesel is produced through a chemical process known as transesterification. Transesterification is a reaction between vegetable oil or animal fat, known as feedstock, and an alcohol (such as methanol). A catalyst such as sodium hydroxide is also employed. A mixture of fatty acid alkyl esters (FAAEs) is the main product and glycerin is a byproduct.[40,41] It is this mixture of FAAEs that is known as biodiesel, as shown in Figure 4. The major component in feedstock for transesterification is triglyceride.

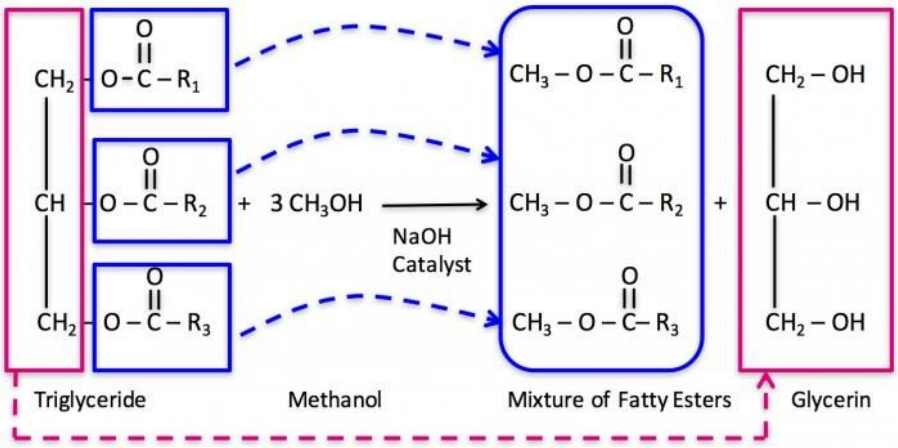

Figure 4. Production of biodiesel via transesterification reaction.[42]

Some relevant variables in the reaction are temperature, time, pressure, catalyst type and concentration, and the feedstock.[41] Some feedstock currently used for biodiesel production include soybean, palm, rapeseed, canola, coconut, cottonseed, sunflower and beef tallow.[22,39,40,43] Table 2 below shows the fatty acid (FA) composition of some common feedstock by weight. Soybean oil is the largest biodiesel feedstock used in the US.[44]

Apart from being renewable and biodegradable, biodiesel is beneficial in so many other ways. Biodiesel has the potential to positively impact the economy by creating new jobs and revenues, especially for rural farmers.[38] Energy crops used as biodiesel feedstock can be used to revegetate barren land and stabilized erosion laden lands, thus creating natural habitats and

Table 2. Fatty acid (FA) composition of common biodiesel feedstock. Linoleic acid represents the most abundant FA in the most used feedstock.

Fatty acid	Shorthand	Soybean	Canola	Rapeseed	Palm	Sunflower
Palmitic acid	C16:0	10.2	4	5.1	42.8	4.8
Stearic acid	C18:0	3.7	2	2.1	4.5	5.7
Oleic acid	C18:1	22.8	60	57.9	40.5	20.6
Linoleic acid	C18:2	53.7	20	24.7	10.1	66.2
Linolenic acid	C18:3	8.6	10	7.9	0.2	0.8
Others		~ 1.0	~ 4.0	~ 2.3	~ 1.9	~ 1.9

improving biodiversity.[30] Another environmental benefit of biodiesel is its reduced GHG, SO_x, CO, HC and particulate matter emissions.[2,30,45] Consequently, there will be a reduction in acid rain.[2] Furthermore, biodiesel can be used in regular diesel engines without any modifications.[40] Biodiesel also contains little amounts of polycyclic aromatic hydrocarbons (PAH) and has a low flash point which makes it safer than petroleum diesel when it comes to storage.[39,40]

Just like many other resources, biodiesel is not without its complications. Although biodiesel has been reported to reduce SO_x and GHG emissions, it contains slightly higher nitrogen amounts than its petroleum counterpart and consequently increases NO_x emissions.[2,45] This can be solved to some extent by pretreating biomass to remove nitrogen, mixing with petroleum diesel or ethanol and employing exhaust filter technology like selective catalytic reduction (SCR) technology.[2,38,46] Biodiesel has also been directly linked to several other environmental problems. One of such environmental problems is land use change which refers to the increase in agricultural land dedicated to producing feedstock for biodiesel consequently resulting in deforestation and the loss of habitats and contributing to the decline of biodiversity.[47] Another environmental concern with biodiesel production is that it necessitates substantial

quantities of water for irrigation and processing, which can place strain on water resources in regions already facing water scarcity.[48] Also, the heightened utilization of fertilizers and pesticides in the cultivation of biodiesel feedstock leads to water pollution, eutrophication, and these have adverse effects on aquatic ecosystems.[49] Another challenge is the fact that biodiesel is expensive to produce which may lead to higher fuel prices for consumers.[50] From the cost of virgin oils to the employment of conversion technologies, the chain of procedures involved in biodiesel production is estimated to be 1.5x more expensive than those of petroleum diesel.[2,22,40,51] However this high cost can be reduced by using low cost feedstocks like waste cooking oils rendered animal fats since most of it is from the cost of virgin oils used for biodiesel production.[40,51] Biodiesel has poor storage stability. In comparison to petroleum diesel, biodiesel has a shorter shelf life and is more susceptible to oxidation, consequently leading to the formation of deposits and potential engine problems, thus requiring the implementation of appropriate storage and handling procedures.[52] Furthermore, a major complication with biodiesel is its operability. Fuel operability is crucial as it dictates the fuel's ability to function effectively under varying operational conditions. It entails the fuel's capacity to perform as designed at specific environmental factors like temperature, altitude, and humidity. Due to biodiesel's high pour point (the lowest temperature that a liquid fuel will flow), it would gel and not perform well in cold temperatures. Treatment methods such as winterization can be employed to reduce its pour point.[53] Another common method for preventing biodiesel gelling is blending it with petroleum diesel. Other ways for improving biodiesel's operability include use of phase change materials (PCM), installing insulating layers on fuel lines, and further refining and filtering.[54] It is also expected that implementing these solutions will further increase costs associated with

biodiesel production and use, and it would consequently lose its economic appeal. Thus, solving the operability problem is key to making it a very suitable alternative to petroleum.

1.5 A Promising Solution: Pyrolysis of FAMEs

The properties of compound are dependent on its molecular structure. It has been found that the length of the hydrocarbon chains and the presence of unsaturated structures significantly affects the properties of biodiesel at low temperatures.[53,55] Thus, shorter chains hydrocarbons and unsaturation conversion technologies should be targeted in the quest to improve biodiesel's operability. However, it is important that structural similarities are preserved. A conversion technology that holds the capacity of breaking long chain hydrocarbons into smaller ones and preserve structural similarity with parent molecule is pyrolysis. Pyrolysis is a process that employs high heating in the absence of oxygen to produce smaller molecular compounds.[38] The absence of oxygen is very critical to the process to prevent combustion. In the case of biodiesel, the products of pyrolysis will be a mixture of shorter chain hydrocarbons in the gaseous, liquid, and solid phases. This mixture of compounds can be separated by fractional distillation based on their boiling points. Pyrolysis as a method for biodiesel processing is advantageous in several ways. Pyrolysis is versatile and offers the capability to process a diverse range of feedstocks, including waste materials and agricultural residues, thereby assisting in mitigating concerns related to feedstock availability.[56] It is also useful in waste reduction. Through efficient conversion of biomass waste streams, pyrolysis can generate valuable energy products, reducing the need for landfill usage and helping to mitigate environmental pollution linked to waste disposal.[57] Pyrolysis holds the capacity to yield multiple energy-rich products and thus can achieve high energy conversion efficiencies. These products can be further utilized or upgraded for various purposes.[56] This leads us to an appealing side to the use of pyrolysis in engineering

fuels that can be a suitable replacement of petroleum as these byproducts hold the capacity to be used for other things that petroleum is used for like polymer production.

However, the use of pyrolysis is not without complications. A major problem of this method is the high capital and operating cost associated with it. Pyrolysis processes can be complex and require advanced technologies for efficient operation, which may further present challenges for scaling up and commercialization.[56]

Since the major objective for employing pyrolysis is to produce shorter chain hydrocarbons, the process can be done on the building blocks of biodiesel – fatty acid alkyl esters (FAAEs). Biodiesel is a mixture of (FAAEs). The type of FAAEs produced is dependent on the short chain alcohol used in the transesterification reaction. When methanol or ethanol is used, fatty acid methyl esters (FAMEs) or fatty acid ethyl esters (FAEEs) respectively. In this theoretical study, a FAME, methyl linoleate, was selected based on its high availability: being the most abundant FAME in the biodiesel mixture from soybean (the most used feedstock in the United States).[39,40,43,44] It is also worthy to emphasize that pyrolysis is difficult to control because of its required high temperature consequently requiring specific equipment and apparatus.[2] Thus, pursuing this research would be expensive. This is a good instance where theoretical investigations as a major driver for cost-effectiveness is needed and appreciated.

1.6 Previous work on Pyrolysis of Biodiesel and Triglyceride

Several researchers have reported their works on pyrolysis of biodiesel. Asomaning *et. al.* (2014) investigated the effects of pyrolysis on transforming polyunsaturated fatty acids into hydrocarbons suitable for renewable chemicals and fuels. Linoleic acid was selected as the representative fatty acid, and a range of pyrolysis experiments were conducted at different temperatures and reaction durations. The resulting gas and liquid products underwent analysis

through gas chromatography and mass spectrometry. The outcomes revealed the generation of CO and CO_2. The gas products comprised alkanes and alkenes in the C1–C5 range, with ethane and propane standing out as the major constituents. Within the liquid portion, n-alkanes, alkenes, cyclic alkanes, alkenes, and fatty acids were found. Ultimately, this study highlights the potential of pyrolyzing polyunsaturated fatty acids to produce renewable hydrocarbons that align with established petrochemical processes. Examining the distribution of products of previous experimental works is vital to this research as it provides a basis for evaluating the accuracy of the adopted computational method.[58]

Lappas *et al*. (2009) discussed the effects of pyrolysis on fuel properties. The study discussed the co-processing of biofuels, including pyrolysis products, with conventional petroleum-based fuels in refining processes. They found that the pyrolysis process can significantly impact the fuel properties of the resulting biofuels. One notable effect is the reduction in the viscosity of the biofuels, making them more suitable for use as transportation fuels. Additionally, pyrolysis can lead to an increase in the energy density of the biofuels due to the formation of shorter-chain hydrocarbons. The chemical composition of the biofuels is also altered during pyrolysis, with a decrease in the content of fatty acid methyl esters and an increase in hydrocarbons such as alkanes, alkenes, and aromatics. Furthermore, the pyrolysis process can enhance the oxidative stability of the biofuels, potentially improving their storage and shelf life.[59] The results from Lappas *et al*. (2009) indicates largely that pyrolysis is a good route to process biodiesel into smaller hydrocarbons that can be potentially used in gasoline engines.

On the other hand, the pyrolysis of triglyceride, the parent material for biodiesel production, is also a rational path to explore in this field. Maher *et al.* (2006) reviewed existing literature on the pyrolysis of triglyceride and divided them into two categories: direct thermal

cracking and catalytic cracking. Thermal cracking studies have shown the generation of complex mixtures of products. However, the specific distribution of these products varies significantly across different studies due to factors such as the type of reactor, residence time, composition of the initial feedstock, reaction temperature, as well as the methods used for collection and analysis. While these studies offer a general understanding of the potential products that can be obtained through pyrolysis, obtaining liquid mixtures with high hydrocarbon content remains challenging due to the presence of undesired oxygenated compounds like carboxylic acids and ketones. For catalytic cracking, four main catalyst types are utilized: transition metal catalysts, molecular sieve catalysts, activated alumina, and sodium carbonate. The resulting reaction products are significantly impacted by both the catalyst type and reaction conditions, leading to a range of fractions resembling diesel and gasoline. Compared to research on biooil and biodiesel, pyrolysis of triglyceride is relatively less advanced, which presents abundant opportunities for further investigation as this research is lacking in areas such as optimization of the reaction conditions to obtain specific reaction products, in-depth characterization of products and their properties, and scaling up the process.[60] However, in their study, Adebanjo *et al*. (2005) have proposed optimal conditions for producing a liquid similar to conventional no. 2 diesel (a distillate fuel oil with a distillation temperature of 640 °F at the 90% recovery point and it satisfies the additional requirements outlined in ASTM Specification D 975.) from the pyrolysis of triglycerides.[61,62] They selected lard as the representative feed material for animal fats due to its easy availability in a pure form. The main goal of the research was to explore the feasibility of producing a diesel-like fuel, as well as other chemicals and high-heating-value gas through lard pyrolysis. The investigation focused on analyzing the impact of temperature, residence time, and particle size of the inert quartz packing on the quality of the liquid product, as well as the

composition and heating value of the resulting gas. The schematic diagram of the experimental setup for this work is shown in Figure 5. They concluded that Lard can be transformed into a diesel-like liquid through pyrolysis without the need for a catalyst, while also generating a high-calorific-value gaseous fuel. The gaseous product primarily consists of C_1 to C_3 hydrocarbons, CO, CO_2, and H_2, whereas the liquid product is composed of various hydrocarbons, aromatics, ketones, aldehydes, and carboxylic acids. The outcome of the pyrolysis process is influenced by temperature, residence time, and particle size in the reactor. Lower temperatures increase the total liquid product, but longer residence times reduce the yield of diesel-like liquid, which is maximized at 600 °C, 1.2 seconds residence time, and particle sizes of 1.7 to 2.4 mm. They found optimal conditions for producing a liquid like conventional no. 2 diesel involve a pyrolysis temperature of 600 °C, a carrier gas flow rate of 5 × 10-5 m3/min (1.8 seconds residence time), and quartz chips with particle sizes of 0.7 to 1.4 mm. This liquid possesses desirable fuel properties, including a cetane index of 46, specific gravity of 0.86, viscosity of 4.5 mPa·s at 40 °C, and a higher heating value of 40 MJ/kg.[61]

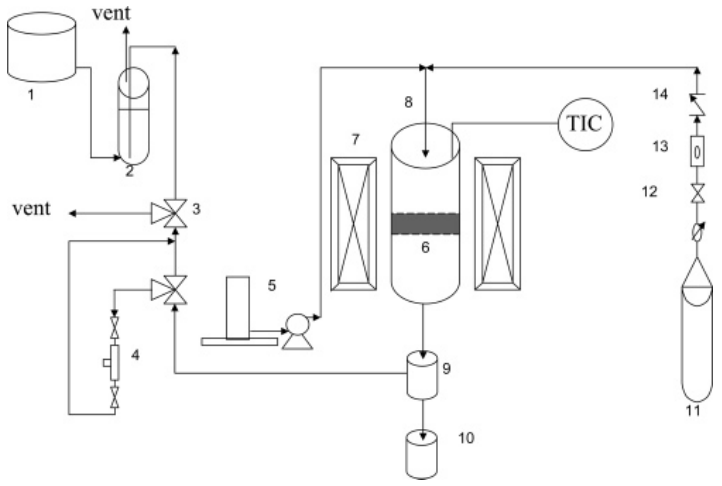

Figure 5. Schematic diagram of experimental setup for pyrolysis of lard: (1) brine solution tank, (2) gas collector, (3) two way valves, (4) sampler, (5) lard feed pump, (6) quartz chips packing, (7) furnace, (8) reactor, (9) ice condenser, (10) condensate collector, (11) nitrogen cylinder, (12) needle valve, (13) mass flow meter, and (14) check valve (Figure 1 from Adebanjo *et. al.* (2005).[61]

1.7 Research Questions and Objectives

The research objectives of this study are threefold. Firstly, the aim is to explore how conventional biodiesel can be enhanced by utilizing pyrolysis to generate low molecular-weight compounds with high energy densities. This will address the limitations of biodiesel, such as its high production costs and poor low-temperature performance. The goal is to break long chain biodiesel molecules into short chain molecules with structural similarities with gasoline that would be functional in gasoline engines. From these dissociations, other alkenes are expected to be produced. These alkenes are very useful as solvents and polymer precursors. Secondly, the study seeks to unravel the pyrolysis path of biodiesel on an atomic scale. By understanding this process at a molecular level, we aim to identify and engineer optimal reactants that maximize the yield of desired energy-producing molecules. To this end, herein we present analysis of an in-house generated database of 100 ab initio trajectories of methyl linoleate to identify significant bond-breaking and bond-forming events, logging their timing and position in the molecule. Thirdly, the methodology employed in this study, as well as in other molecular dynamics research, has highlighted the necessity of automating certain aspects of post-simulation analysis. Using large sample sizes is crucial to the accuracy of theoretical results. A computer-based analysis method (CBAM) is currently being developed and tested by comparing its results with analysis results from the conventional human oriented visual analysis method. Through these objectives, the research aims to contribute to the development of improved biodiesel and advance our understanding of the pyrolysis process at an atomic scale.

CHAPTER 2: COMPUTATIONAL METHODS IN CHEMISTRY

2.1 Computational Chemistry

Computational chemistry use simulations to model echemical reactivity.[63,64] Such computer based simulations serve as a compliment to conventional experiments and present an oppurtunity to make discoveries before applying methods experimentally and on a large scale. Consequently, this reduces the costs associated with research.[63,65] Although computational chemistry research would not have expenses related to purchase of chemical supplies and chemical waste disposal, it still has its costs that include talent training, performance, data storage in addition to computer hardware, and time consumption.[65] Computational chemistry serve as a bridge between the microscopic world of the building blocks of matter and the macroscopic world of laboratory experiments and observations.[66] Figure 6 illustrates how computer simulations compliment experinmental work.

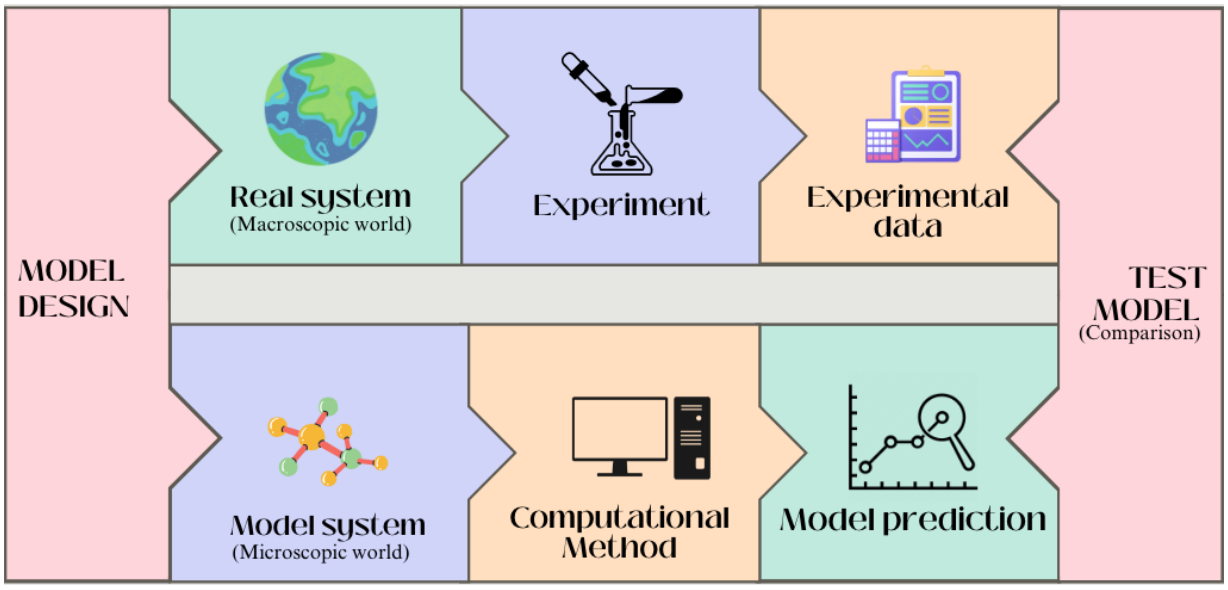

Figure 6. A graphic illustration of the complimentary relationship between experiments and computational modeling in the study of matter.

In most cases, computational chemists study the structure, potential energy surface, and chemical properties of a system. The structure would entail the atomic compostion of the molecule, and how they are connected in space. Potential energy surfaces will be decribed in the next section. The chemical properties determined by computer simulations can be further divided into three: single-molecule properties (i.e., properties that are measurable from one molecule, examples include spectroscopic quantities like nuclear magnetic resonance); molecular energetics (equilibruim constants, heats of formation and combustion, etc.); and 'non-physical-observable' properties such as bond order and aromaticity, which have been proven to aid understanding of chemical systems.[65]

2.2 Potential Energy Surfaces (PESs)

In a conventional laboratory experiment, reactants and products most often are a mixture of isomers or similar molecules. Since chemical simulations are supposed to model experimental chemical environment, it is crucial that simulations make room for other possible structures and geometries of the molecules in the system of study. A molecule is comprised of atoms and bonds, and as geometry changes, atom positions and bond lengths change. If we view this in the macroscopic world with atoms as balls and bonds as springs, in the new geometry, the balls (or atoms) are relatively motionless, thus the molecule has a new potential energy. The concept of a PES is very critical to the subject of computational chemistry as it allows for calculation of the repective potential energies when molecules attain new geometries as forces are applied. A PES is a graph of the potential energy as a function of atomic position or can be in the form of a data table or an analytical function that provides the energy associated with any position of the nuclei in a chemical system.[67,68] Although the behavoir in the microscopic world of real atoms and bonds are similar, a major way these views differ is that real atoms and bonds are constantly

vibrating. Figure 7 shows the PES for a diatomic molecule in both macroscopic and microscopic worlds.

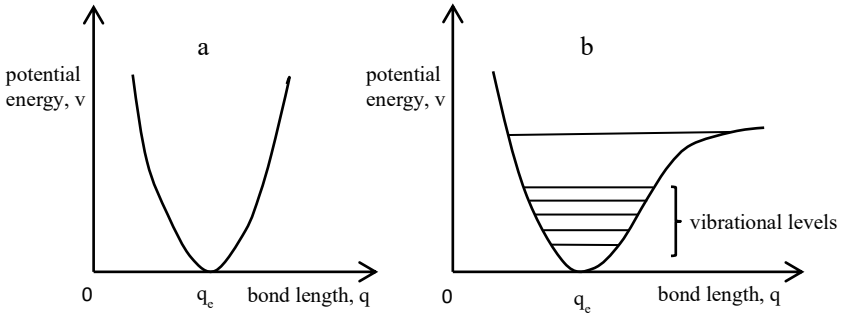

Figure 7. Potential energy surfaces for a diatomic molecule in the described (a) macroscopic world with the balls-and-spring model of a diatomic molecule in its normal geometry, q_e, if we stretch or compress the "bonds" by grasping the "atoms," the potential energy of the molecular model increases, and is approximated with a quadratic curve; and (b) real microscopic world. Actual molecules occupy vibrational levels. When the bond length q is either stretched or compressed away from its equilibrium value q_e, the potential energy increases to a certain extent, upon which the potential energy deviates from the quadratic curve.[67]

Molecules with more than two atoms would increase the dimensions of the PES curves. For example, water (H_2O) with three atoms (N) would have nine variables (3N) to describe its position in three-dimensional space. While the '3N' model would lead to more complications, especially with bigger molecules, another problem is that this expression does not provide a unique definition of the structure because it relies on an arbitrary origin.[65] We can solve this problem by adopting an internal coordinate description of the molecule. Internal coordinates describe the relative positions of atoms within a molecule. They are referred to as "internal" because they reflect the molecule's internal geometry by describing the position of each atom in terms of its distance and angle relative to other atoms in the molecule. Choosing the first atom fixes the origin and does not involve any geometric degrees of freedom. The position of the second atom is uniquely defined by its distance from the first, meaning that a two-atom system has only one degree of freedom which is the bond length as shown in Figure 8. To specify the

position of the third atom in a molecule, it must be described either by its distances to each of the preceding atoms or by a distance to one and an angle between the two bonds defined so far to a common atom. A three-atom system, assuming collinearity is not imposed, possesses three degrees of freedom. The introduction of an additional atom would require three coordinates to define its position within the molecule. Figure 8 provides a graphic depiction of the internal coordinates for a molecule with one atom and molecules with more than one atom up to four atoms and their respective degrees of freedom.[65]

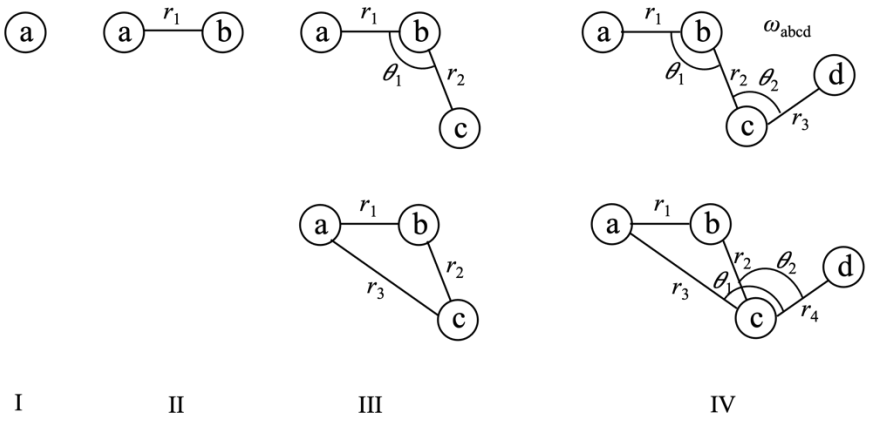

Figure 8. Graphic depiction of different means of specifying internal coordinates. **(I)** A system with only one atom and no degree of freedom. **(II)** A system with two atoms with one degree of freedom: bond distance, r_1. **(III)** A system with three atoms. The position of the third atom requires two additional degrees of freedom, which can be specified as either two bond lengths (r_2 and r_3) or a bond length(r_2) and a valence angle (θ_1). **(IV)** A system with four atoms. The position of the fourth atom requires three additional degrees of freedom: bond length (r_3), a valence angle (θ_2), and a dihedral angle(ω_{abcd}); or a bond length (r_4) and two valence angles (θ_1 and θ_2). The choice of how to specify the molecular geometry is usually a matter of computational convenience.[65]

PESs with three degrees of freedom to consider (along with energy) are referred to as hypersurfaces, and can be called potential energy hypersurfaces.[67] As the dimensions increase, the problem becomes more complex. This leads to the n-body problem. In computational chemistry, the n-body problem pertains to the task of predicting the behavior of a system

consisting of n particles such as atoms or molecules, which interact through mutual forces. The problem requires determining the positions and velocities of all the particles in the system, based on their initial conditions and the fundamental laws of physics that dictate their interactions.

After computing a Potential Energy Surface (PES), it becomes possible to extract valuable information regarding the chemical system. This comprehensive description takes into account all conformers, isomers and energetically accessible motions of the system. The minima on the PES represents optimal molecular structures, with the lowest-energy minimum referred to as the global minimum (Figure 9). Several local minima, including higher-energy conformers and isomers, may also exist (Figure 9). The maximum on this surface represents the transition states between the reactants and products of a reaction.[65,68]. In the case of higher dimensional PESs, or hypersurfaces, the diagram becomes complex and many concepts not expressible in a one-dimensional PES can be expressed (Figure 10).

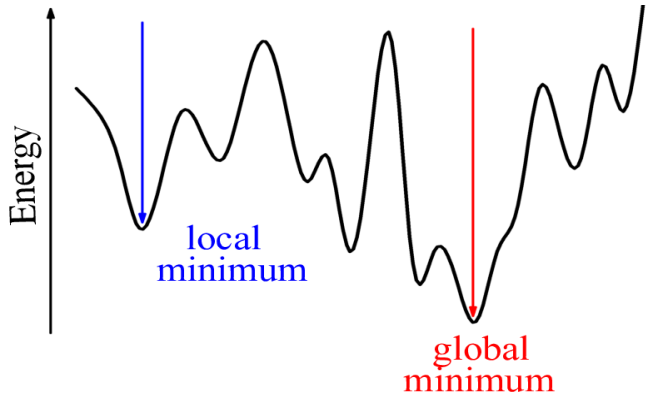

Figure 9. Graphic illustration of a one-dimensional potential energy surface.[69]

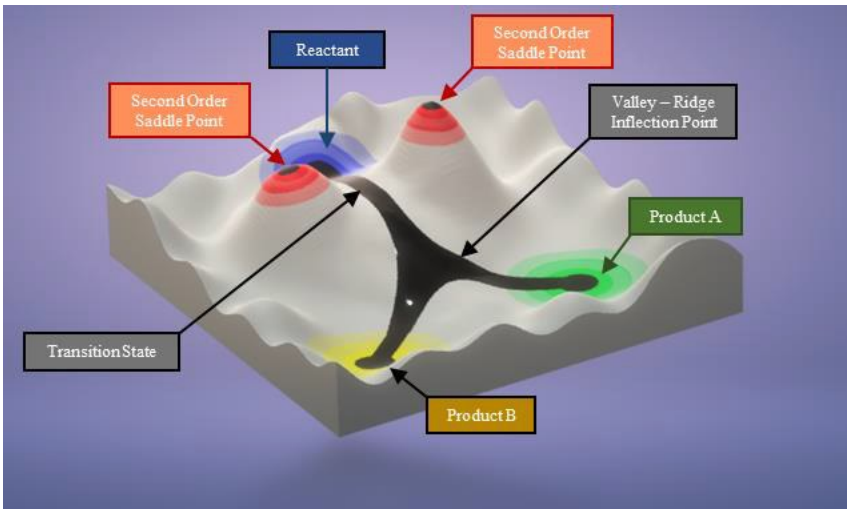

Figure 10. Potential Energy Surface of a two-dimensional system.[22]

2.3 Electronic Structure Theory

Electronic structure theory refers to a collection of computational and theoretical techniques used to investigate the electronic structure of molecules, atoms, and solids. It endeavors to comprehend the spatial arrangement of electrons and their energies in these systems, which is crucial for comprehending their physical and chemical properties. Electronic structure theory is based on the principles of quantum mechanics and utilizes mathematical models and algorithms to solve the Schrödinger equation, which explains the behavior of electrons in a specific system. The Schrodinger equation can be expressed in two forms: time-independent (Equation 3) and time-dependent (Equation 4).[22]

$$\hat{H}\Psi = E\Psi \tag{3}$$

$$\hat{H}\Psi(x,t) = i\hbar\frac{\boldsymbol{\delta}\Psi}{\boldsymbol{\delta t}} = \hat{E}\Psi(x,t) \tag{4}$$

The Schrodinger equation uses the Hamiltonian operator ($\hat{H}$) on the wavefunction (Ψ). $\hat{H}$ uses a potential energy operator and a kinetic energy operator (Figure 11) to express the total energy of the system.

$$\hat{H} = \sum_{n=1}^{N} \hat{T}_n + \hat{V}$$
$$= \sum_{n=1}^{N} \frac{\hat{\mathbf{p}}_n \cdot \hat{\mathbf{p}}_n}{2m_n} + V(\mathbf{r}_1, \mathbf{r}_2, \ldots, \mathbf{r}_N, t)$$
$$= -\frac{\hbar^2}{2} \sum_{n=1}^{N} \frac{1}{m_n} \nabla_n^2 + V(\mathbf{r}_1, \mathbf{r}_2, \ldots, \mathbf{r}_N, t)$$

Figure 11. Hamiltonian operator expressed as a function of the potential and kinetic energies of the system. The potential energy operator ($\hat{V}$) is a function of spatial configuration of the system and time.[70]

It is worthy of note that the Hamiltonian operator would take geometry inputs (x, y, z positions in a 3D cartesian space) of both nuclei and electrons (subatomic particles) for its solution. This is because the potential energy operator ($\hat{V}$) shown in Figure 11 is a function of the spatial configuration of the system. So for a molecule such as water with 10 electrons and 3 nuclei, the potential energy operator will take in 39 spatial variables in the form:

$$\hat{V} = V(r_{1x}, r_{1y}, r_{1z}, r_{2x}, r_{2y}, r_{2z}, r_{3x}, r_{3y}, r_{3z}, \ldots, r_{13x}, r_{13y}, r_{13z}) \quad (5)$$

A mathematical description of the Hamiltonian operator takes the form:

$$\hat{H} = T_e + V_{ee} + V_{eN} + T_N + V_{NN} \quad (6)$$

where the terms represent the electronic kinetic energy (T_e), the electron–electron Coulombic repulsion (V_{ee}), the electron–nuclear Coulombic attraction (V_{eN}), the nuclear kinetic energy (T_N) and the nuclear–nuclear Coulomb repulsion (V_{NN}), respectively.[71] In order to reduce the complexities encountered in modeling systems with large numbers of atoms, several approximations have been made. One of the approximations used in electronic structure theory is the Born-Oppenheimer (BO) approximation. The BO approximation assumes that the nuclei are essentially stationary compared to the electrons. This approximation is very vital to computational chemistry as it simplifies the Schrodinger equation as we can focus on the

electronic energy and add a nuclear portion later to account for internuclear repulsion. By using the Born-Oppenheimer approximation, the kinetic energy of the nuclei is assumed to be zero, and electron-nucleus correlation is neglected, thus simplifying the Hamiltonian operator. Consequently, only the first, second and third (which becomes a constant) terms remain in the operator.[72] It also sets a precedent why the PES diagram is a plot of energy against nuclear coordinates rather that electron coordinates because the attractive forces between the cloud of mobile elctrons and the nuclie locks the nucli to a specific position and reveals the local positions of the atom (or atoms in the molecule) at that time. This is what makes for the geometry of the system. In the macroscopic world, the structure of a molecule influences the properties of that molecule. This is the case for geometries in models: they have significant impact on the molecule's properties. It is a natural phenomenon that molecules will preferenntially adopt configurations of lower energy (most stable). Therefore, determining the most stable geometry is important in understang and predicting the properties of matter. This is known as geometry optimization. Initially, the user needs to specify the molecular geometry of the molecule. Subsequently, the program calculates the energies and energy gradients to identify the molecular geometry that corresponds to the minimum energy.[67,68] Discovering the lowest energy structure allows for identifying the most stable geometry of the molecule, which helps to make predictions about its properties.

Although we achieve a relatively high level of simplicity with the Born-Oppenheimer approximation, there is still a complexity problem. The repulsion between every electron (the second term in Equation 6) is a challenging problem to solve for many-body systems. The Hartree-Fock (HF) approximation addresses this challenge by approximating each electron as a single electron orbital. The HF approximation takes into account the electron-electron repulsion

by approximating the repulsion terms in the Schrodinger equation as an average iteration between electrons.[22,65] This approximation is advantageous in that it simplifies the many-electron Schrödinger equation into multiple one-electron equations.[68]

2.4 Molecular Dynamics and *Ab Initio* Molecular Dynamics

Molecular dynamics (MD) simulation is a computational method that allows for a very fine microscopic modeling done on a molecular scale.[63] MD studies the movements, deformations and interations of molecules over time by solving equations of motion and generating a dynamic visual representation of the occurences in the system.[63,73,74]

$$F = ma \tag{7}$$

The accuracy of a MD calculation heavily depends on the method used for defining the forces.[71] In various applications, forces are computed using an empirical model or "force field," which has been widely successful in describing a broad range of systems, including simple liquids, solids, polymers, proteins, membranes, and nucleic acids. However, force fields typically do not incorporate electronic polarization effects and may require specialized techniques to handle chemical reactivity. Therefore, for more precise treatment of these effects, *ab initio* MD (AIMD) methodology is often necessary.[71] Also, most MD models used for studying molecules with large numbers of atoms are reported to be classical and for a classical system, Newton's second law of motion (Equation 7) represents the simplest of the equations of motion.[22,73] The reason for using classical mechanics instead of quantum mechanics, especially as the latter provides a finer description of the behavior of matter, is because the solution of the Schrodinger equation becomes more and more complex as the number of atoms in the molecule increases.

The term *ab initio* is latin for "from the beginning" and it is used to refer to computational methods built up from fundamental physical principles without any experimental

data.[68] Classical molecular mechanics and AIMD have distinct domains of application. While classical mechanics is suitable for describing large systems (> 100 atoms), AIMD calculations are restricted to small molecular systems (< 100 atoms) due to their demanding quantum mechanical analysis, consequently resulting in significantly higher computational costs. Although AIMD calculations are more expensive, it is advantageous as it provides a finer description of the system. At the core of every *ab initio* molecular dynamics method lies the concept of calculating the forces acting on the nuclei using electronic structure calculations that are conducted in an "on-the-fly" manner while generating the molecular dynamics trajectory.[71,75] This allows chemical bond breaking and forming events to occur and accounts for electronic polarization effects.[71]

2.5 Density Functional Theory (DFT)

In recent years, Density Functional Theory (DFT) has gained significant popularity and has become the electronic structure method most commoly used in AIMD.[22,68,71] This can be attributed to it being less computationally demanding compared to other methods with similar levels of accuracy.[68] Density functional theory (DFT) is a computational method that uses the electron density rather than the wavefunction to make predictions about the properties of molecular systems.[76] Density Functional Theory (DFT) operates on the premise that the energy of a molecule can be derived from its electron density rather than its wave function. This is based on the Hohenberg-Kohn theorem that states that the electron density function of an atom or molecule determines its ground-state properties. Although Hohenberg and Kohn stated this, a practical application of this thoery similar to the Hartree-Fock method was developed by Kohn and Sham.[67,68] In DFT, the total energy of a system is expressed as a functional of its electron density, rather than being calculated from the complex N-electron wave function, as in

traditional methods.[67] Figure 12 provides a pictoral illustration of both methods and how they differ. The electron density is calculated by solving the Kohn-Sham equations. These equations simplifies the challenging problem of the many-body system involving interacting electrons in a static external potential to a manageable problem of non-interacting electrons that move in an effective potential. The effective potential comprises the external potential and considers the influence of Coulomb interactions between the electrons, including exchange and correlation interactions.[77,78]

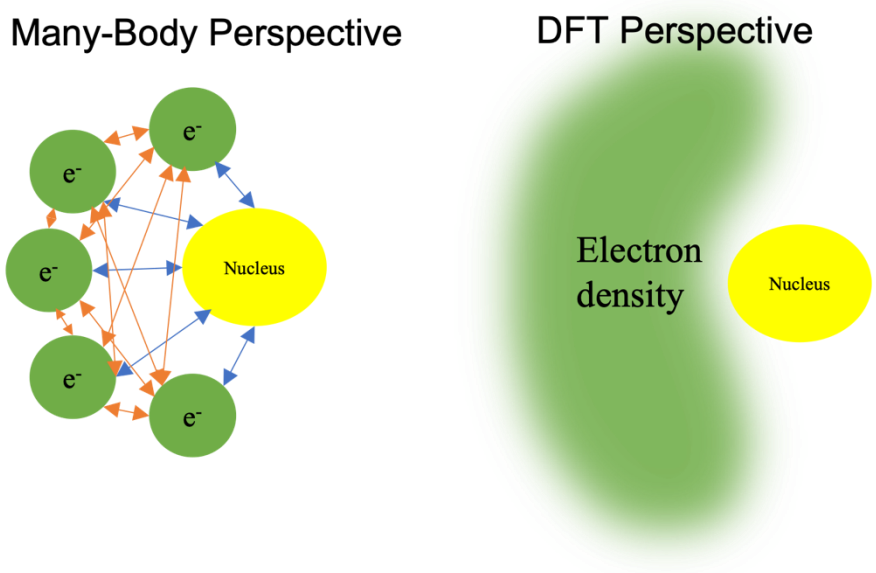

Figure 12. A graphic illustration of Many-Body perspective vs DFT perspective. DFT replaces the many particle electron idea with electron density. The blue arrows represents attractive coulombic forces between the nucleus and electrons; the red arrows represents repulsion between electrons.

DFT has many advantages such as its computational efficiency and its ability to capture many-body effects. However DFT has some limitations. In DFT, the self-interaction error (SIE) arises when a single electron in the electronic density functional interacts with itself. In principle, this interaction should cancel out, as an electron cannot interact with itself. However, the exchange-correlation functionals utilized in DFT do not accurately account for this cancellation,

leading to potential overestimation or underestimation of the energy and electronic properties of a system. As a result, errors may arise in predicting chemical reactions, electronic structure, and other relevant properties. To address this issue, researchers have developed several correction methods, including the use of hybrid functionals that blend DFT with other techniques like Hartree-Fock.[79,80] A delocalization error also arises in DFT when the energies of delocalized systems (such as molecules with extended pi systems or metallic systems) are underestimated.[81] These type of errors can also be corrected by using hybrid functionals. Dispersion error in DFT arises from the fact that the exchange-correlation functionals used in DFT do not accurately account for van der Waals forces, which are crucial in the interaction between atoms and molecules. When this error is not corrected, the accuracy of DFT can be affected. To tackle this problem, dispersion-corrected DFT methods have been developed, which incorporate corrections for dispersion interactions.[77,78]

2.6 The Concept of an Ensemble and its Importance

In computational chemistry, an ensemble refers to a collection of multiple molecular structures that represent the different possible conformations or configurations of a molecule or a system of molecules. In the macroscopic world, the focus of the majority of chemical research is not on a single molecule, but rather on observable macroscopic properties of matter that consist of incredibly large numbers of molecules – an ensemble.[65] Various laboratory experiments and syntheses reveal several products including a mixture of regioisomers, stereoisomers and compounds with different vibrational states. What this points to is that reactions may proceed in several pathways. The importance of using ensembles in computational chemistry is to capture all possible pathways of a reaction. Ensembles can more accurately capture the dynamic behavior of molecules and the impact of conformational changes on their properties and

interactions with other molecules by taking into account multiple conformations. The most realistic depiction of how a reaction occurs is through an ensemble of trajectory calculations.[68]

CHAPTER 3: RESEARCH METHODOLOGY

3.1 AIMD Database Human-Oriented Visual Analysis (HOVA)

The previous chapter discussed molecular dynamics and approximations used in *ab initio* molecular dynamics in a general sense. However, this chapter discusses *ab initio* molecular dynamics as it was used specifically for this work. To begin, an overview of what the steps in *ab initio* molecular dynamics simulation entail is given below:[68]

1. **Selection of System**: The initial step in *ab initio* molecular dynamics involves selecting a system of interest and determining its initial state, which includes specifying the positions and velocities of its constituent atoms.
2. **Calculation of Potential Energy**: Subsequently, the potential energy of the system is computed based on the electronic structure of the atoms. The calculation is typically carried out using quantum mechanical methods such as density functional theory (DFT) or other suitable techniques.
3. **MD Simulation**: Following the calculation of potential energy, the system is simulated using molecular dynamics (MD) techniques. The MD simulation involves updating the positions and velocities of the atoms based on the forces acting on them for a short time (timestep), which is achieved by solving the equations of motion for the atoms.
4. **Repeat Cycle**: The process outlined in steps 2 and 3 is repeated for a specified number of time steps or until a specific stopping criterion is met. In our case, it was an average of 1000 time steps. During the simulation, properties of the system, such as its energy, temperature, and pressure, can be monitored and analyzed.

5. **Post-simulation Analysis**: Following the simulation, the trajectories of the atoms can be analyzed to extract various properties of interest, such as diffusion coefficients, reaction rates, and structural properties.

In computational chemistry, a model chemistry refers to a set of theoretical methods and approximations used to calculate the electronic structure of molecules or materials. The choice of model chemistry can greatly affect the accuracy of the computed properties, such as energies, structures, and spectroscopic properties. Model chemistries typically include a combination of a funtional and a basis set. The functional describes the approximate exchange-correlation energy of the electronic system, while the basis set describes how the wavefunction is represented in terms of atomic orbitals.

Pierre Hohenberg and Walter Kohn proposed that the energy of a system could be expressed in terms of the electron density functional, as shown below:

$$E[\rho] = T_s[\rho] + J[\rho] + E_{xc}[\rho] \quad (7)$$

Where $E[\rho]$ is the energy of the system, $T_s[\rho]$ is the kinetic energy of the non-interacting system, $J[\rho]$ is the electrostatic distribution of the charge, and $E_{xc}[\rho]$, known as the exchange-correlation functional, is the information that is not known about the system. It should be noted that a functional is a function that takes another function as its input. It is this exchange-correlation functional, which is unknown, that is being approximated by trying out various functional methods.[76]

On the other hand, a basis set is a collection of mathematical functions, known as basis functions, which are employed to approximate the electronic wavefunction or density (as appropriate). This technique is commonly used in the Hartree-Fock method and density-functional theory to convert the partial differential equations of the model into algebraic

equations that can be efficiently solved on a computer. By combining the basis functions in a specific way, the electronic wave function can be represented as a linear combination of these functions, allowing for a computationally feasible description of the electronic structure. The selection of an appropriate basis set is crucial to accurately represent the electronic wave function, and a wide range of basis sets are available with varying levels of accuracy and complexity. The basis set is usally composed of atomic orbitals and there are different types of orbitals that can be used. STOs (Slater-type orbitals) were initially used as basis functions for computational chemistry. However, it was found that performing integrals using STOs is computationally challenging. Frank Boys proposed approximating STOs as linear combinations of Gaussian-type orbitals (GTOs) instead. GTOs allow for closed-form integrals, as the product of two GTOs can be expressed as a linear combination of GTOs. This approach, which was pioneered by John Pople, results in significant computational efficiency and has become a widely used approach in computational chemistry.[77,78,82] Both the functional and basis set are chosen to approximate the true wavefunction of the electronic system, and different combinations of functional and basis set can be used to achieve different levels of accuracy in the calculation. In fact, these two represent the biggest factors in determining the accuracy of the results.[68]

In a previous work, Wilson and Siebert selected a model chemistry that best reproduces experimental BDEs of 44 reactions (chemical moiety representatives – CMRs) that had structural resemblance to methyl linoleate and methyl oleate.[83] The results of the work were collected for direct molecular dynamics simulations, which will accurately account for kinetic and thermodynamic properties of the system. One such property is the vibrational energy of the atoms in the large molecule. The selected model chemistry was M06-2X/6-31+G(d,p), in the format of FUNCTIONAL/BASIS SET. The M06-2X functional belongs to a group of highly

parametized approximate exchange-correlation energy funtions called Minnesota Functionals (Myz).[84] The M06-2X represents the top performer within the 06 functionals (a family of functionals within the Myz group) for main group thermochemistry, kinectics and non-covalent interactions (like hydrogen bonding, π-π stacking, and van der Waals forces).[84,85] The 6-31+G(d,p) is a double-zeta basis function which means it has two basis functions per valence orbital.[86] The method was chosen based on degree of alignment with experimental BDEs of the CMRs as well as the economy of usage.[72] Consequently, the model chemistry is used for *ab initi*o molecular dynamics (AIMD) simulation to generate a database of 100 trajectories for analysis. Figure 13 below is a picture of a typical methyl linoleate initial state used to simulate a trajectory in the database.

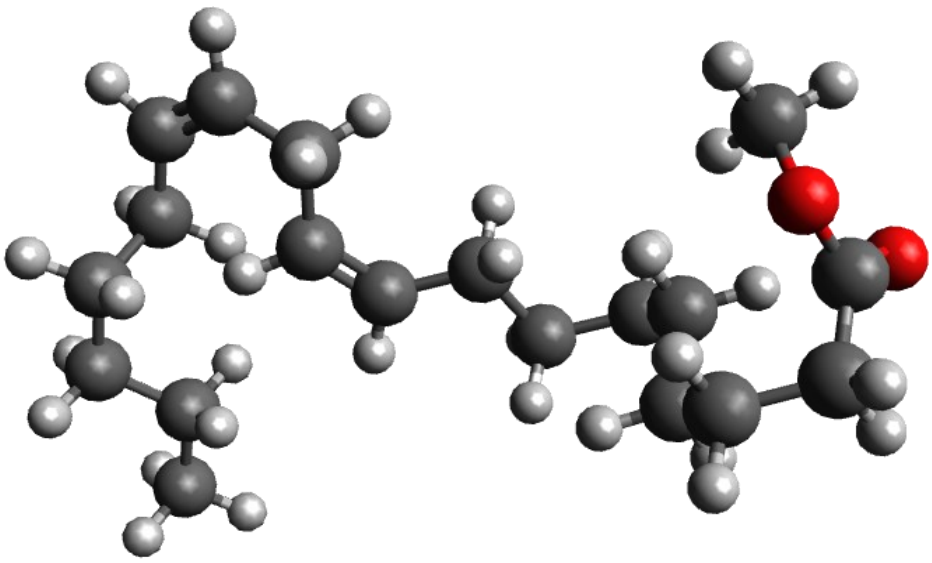

Figure 13. A typical methyl linoleate trajectory in the AIMD database. The colors red, dark grey, and light grey represent oxygen, carbon and hydrogen atoms respectively.

Figure 13 above is a picture of what a methyl linoleate trajectory looks like. However, a trajectory is a movie in which atoms receive new positions every discrete timestep. This new

position of atoms are determined by solving Newton's law of motion. Trajectories in our database had a time step of 1.0 fs with an overall timeframe of 1000 fs. All trajectories (movies) were watched for bond- breaking and bond-forming events, and the time of occurrence of the events were logged.

3.2 Test for Statistical Significance

Computational methods are characterized by approximations. These approximations may indirectly reduce the accuracy of findings. Also, the thermal cracking process is characterized by homolytic scissions. Homolytic scissions in turn leaves two radicals behind. Free radicals are known to be very reactive and thus they have very short life span. The trajectories in the AIMD database show the fate of these radicals over the set time allocation. It is pertinent to note that such high energy systems have high entropy (or degree of randomness) and as such, some events may be due to random chance. To eliminate this possibility to a reasonable degree, a statistical significance test is done. An event (or observation) is said to be statistically significant if it is unlikely that it happened due to random chance. A test for statistical significance is a method used in statistical analysis to determine whether an observation is likely to be real or simply due to chance. In conducting this test, a hypothesis is first made that postulates that there is no real difference between the groups being examined. This hypothesis is known as the null hypothesis. The test calculates a p-value, which is a measure of the probability that the observed difference or effect could have occurred by chance alone. A pre-determined threshold, called the confidence level, is set. A critical value (Z score) is obtained from a probability distribution based on the threshold set. If the p-value, is lower than a pre-determined threshold (α, typically 0.05), then the null hypothesis is rejected, and it is concluded that the difference or effect is statistically significant. In this work, the confidence level was set to 95%, resulting in a critical value of 1.96.

Figure 14 provides an illustration for this. Expressions of statitical equations for this test can be seen in Equation 8 and Equation 9.

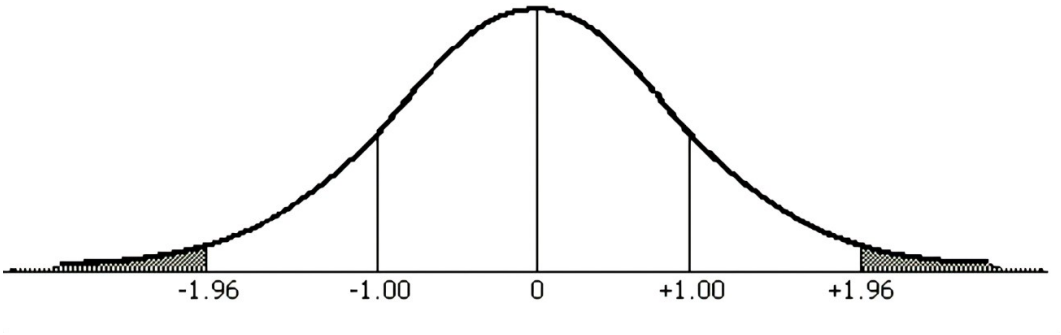

Figure 14. Standard Normal Distribution curve at 95% confidence level (α is 0.05). The null hypothesis can be rejected if the p-value is within the shaded area.[87,88]

For event x,

$$Pr(x) = \frac{N_{obs(x)}}{N_{total}} \tag{8}$$

$$CI = Z\sqrt{\frac{Pr(x)\times[1-Pr(x)]}{N_{total}}} \tag{9}$$

Where Pr(x) is the probability of event x occuring, which is given by its frequency per total number of events that occurred; CI represents confidence interval; and Z represents critical value (or Z score – 1.96 in this test).

After watching the trajectory movies and logging the events, a test for statitistical significance was done to get only significant events. However, the results of this test can be influenced by the sample size because larger sample sizes provide greater statistical power and can result in more significant results.

3.3 Bond Dissociation Energy (BDE) Calculations

One important aspect of chemical behavior is the bond dissociation energies (BDEs) associated with its molecular structure. By understanding the specific BDEs, researchers can gain

a better understanding of the underlying chemical processes involved in its transformation and utilization. BDE refers to the energy necessary to break a chemical bond. It measures the strength of a chemical bond and represents the energy required to break the bond homolytically, where each atom retains one electron of the shared pair, under specific conditions. The unit of measurement for BDE is typically expressed in kilocalories per mole (kcal/mol). The significance of BDE calculations in AIMD lies in the valuable information they provide regarding the stability and reactivity of chemical compounds. In AIMD, BDE calculations enable the investigation of the breaking and formation of chemical bonds in real-time, which is essential in this work for comprehending chemical reactions and reaction mechanisms. Also, since the primary path of pyrolysis is homolytic bond cleavages, BDE calculations are vital in the description of the system being investigated.

For the reaction below:

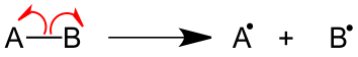

(10)

Let…

$$E_{AB} = EE_{AB} + ZPEC_{AB} \tag{11}$$

$$E_{A\cdot} = EE_{A\cdot} + ZPEC_{A\cdot} \tag{12}$$

$$E_{B\cdot} = EE_{B\cdot} + ZPEC_{B\cdot} \tag{13}$$

Then…

$$BDE = 627.51(E_{A\cdot} + E_{B\cdot} - E_{AB}) \tag{14}$$

Where EE and $ZPEC$ represents the electronic energy and zero-point energy correction repectively, in hartrees (Ha). 627.51 kcal/mol is equal to 1 Ha and is used as a conversion factor in Equation 13. Therefore, BDE is expressed in kcal/mol in Equation 13. Both EE and $ZPEC$ are computed with the *Guassian* 09 Suite.[89] The Zero-Point Energy is the lowest energy state that a

molecule can have as a result of its vibrational motion, even when the temperature is at absolute zero. The Zero-Point Energy Correction is a correction term used in computational chemistry to account for the quantum mechanical effects of these vibrations. ZPEC is significant contributor in the calculation of a molecule's total energy. Neglecting this correction may lead to inacurate energy calculations and, consequently, an incorrect prediction of its properties.[68,90]

Several studies, mostly computational, have shown BDE information for various FAMEs. This is important to this work as it provides a point of reference for determining the accuracy of the model chemistry employed in this work. Siebert and Wilson have reported BDEs for methyl linoleate and methyly oleate. In this study, they utilized various quantum chemical methods, such as B3LYP, M06-2X, B97D, MP2, and CBS-QB3, to investigate BDEs. To evaluate the accuracy of these methods, a set of 44 reactions, reffered to as chemical moeity representatives (CMRs), with known experimental energies were focused on. These CMRs were chosen based on their structural similarity with FAMEs. The results indicate that the M06-2X/6-31+G(d,p) model chemistry is more cost effective and yields close results comparable to the experimental BDEs of the CMRs. This provides a basis for a cost-effective alternative for estimating BDEs in similar systems. Figure 15 below is a methyl linoleate trajectory with BDEs indicated for each bond.[83] In the next chapter, the BDEs determined by Wilson and Siebert will be compared with the BDEs of bonds that cleaved in the first event.

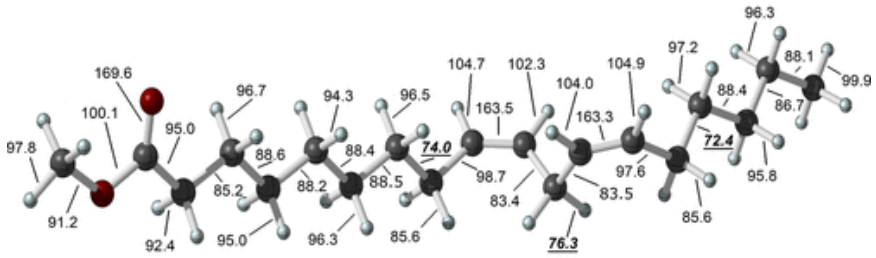

Figure 15. M06-2X/6-31+G(d,p) optimized geometry of methyl linoleate with BDEs for each bond, in kcal/mol. Preferred sites for bond cleavage are indicated in ***bold, italic, and underlined*** text.[83]

3.4 Development of Computer-based Analysis Method

Understanding the methodology of this work, and many other molecular dynamics work, has led to a need to automate some portion of the post-simulation analysis. The importance of creating an ensemble and large sample sizes have been discussed in previous sections. This points to the fact that we need large ensembles for more accurate description of our system. In this work, a total of one hundred (100) trajectories were analyzed for bond breaking and bond forming events. The conventional way of analysis is a human-oriented visual approach (HOVA) where a person sits to "watch" the movies and manually logs the events as he or she sees them occur. To increase accuracy of the system we seek to understand and describe, a larger ensemble with more trajectories is required. The problem with this is that the human oriented approach analysis of larger ensembles would be more time consuming and prone to a higher degree of human error. It then becomes important to automate "watching" with computational means. This has led to the development of a computer-based automated analysis method. Figure 16 gives an illustration of the steps taken in the development of this method.

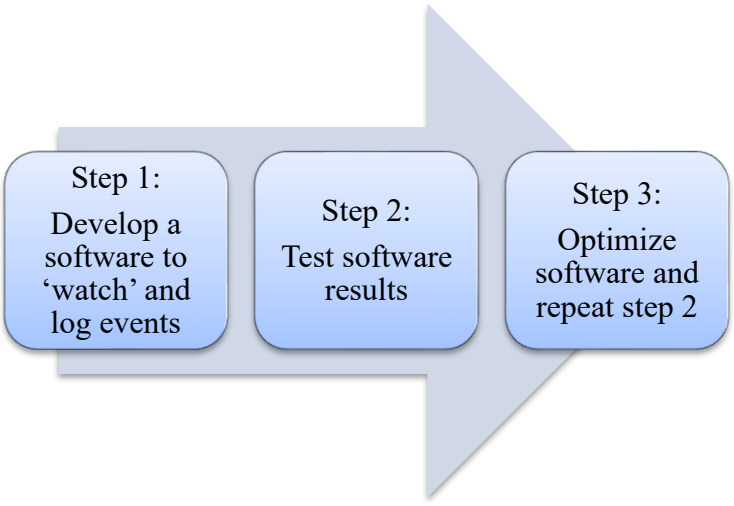

Figure 16. Steps taken in developing computer-based automated method for complete trajectory analyis.

The first step of developing the software (done by another part of the Siebert lab) involved using a lot of python libraries. The software was writen in python language and some of the libraries used include ASE (atomic simulation environment), numpy, pandas, and gaussian 1D filter. There are two types of events to be logged: breaking events and forming events. For the purpose of understanding what the computer does in this method, a cursory outline of steps taken by the computer to log breaking events is given below:

1. Create a list of atom pairs indices (x and y) where bonds exist
2. Get a list of the velocity (distance per time) of the pairs at every timestep. Atoms are in constant vibrations and move some distance naturally without any external force. Thus, only distance would not adequately define bond cleavage. But if a pair of atoms that were bonded move relatively far apart from each other in a relatively shorter time, it is very likely that bonds were broken.
3. Iterate through the list in step 1 and fish out atom pairs that have velocities above a certain threshold.
4. Get the timestep (t) where this velocity that is above the threshold is first observed.
5. Return a list with the index of the pairs and the timestep. It takes the form of [‘b’, x, y, t], where ‘b’ signifies that it is a breaking event.

Below is a cursory outline of the steps taken to log forming events:

1. Create a list of the indices of pairs of non-bonded atoms (x and y).
2. Get a list of the distances between the atoms (x and y) at every timestep.
3. Iterate through the list in step 1 and calculate the covalent radii factor of these atoms. The covalent radii factor is a function of the sizes of the atoms and a determined constant. The next section explains in detail the function of Van der Wall radius in

determining the specific interatomic distance below which a bond is considered to have been formed.

4. Get the timestep (t) where the distances in the list in step 2 is less than or equal to the covalent radii factor calculated in step 3.
5. Return a list with the index of the pairs and the timestep. It takes the form of [‘f’, x, y, t], where ‘f’ signifies that it is a forming event.

In determining forming events, one other thing that is considered is the possibility of a rebreak. Thus if two events occur between same atoms such that one event is a forming event and the other is a breaking event, the computer would not log either of them. The returned list is generated for every trajectory and is stored in a dataframe, and eventually exported as a csv file. The software also returns the fragment products per trajectory.

The software was tested with the AIMD trajectory database and the results were compared with the results from the visual analysis. Based on the results, we improve the code and repeat testing.

3.5 Van der Walls Radius

A very crucial part of thermal cracking studies is the determination of the point where a bond can be considered broken or formed. To determine the breaking or forming of a bond in computational chemistry, the distance between the two atoms forming the bond is monitored. The bond is regarded as broken when the distance between the atoms exceeds a defined threshold value or is regarded as formed when the distance between the atoms goes below a defined threshold value. The Harmonic oscillator potential and the Morse potential are models that describe the bond energy as a function of internuclear distance (bond stretching).[68] However, the Morse potential provides a more precise depiction of a molecule's energy as it accounts for

the anharmonicity of molecular vibrations (specifying that vibrational energy levels are not equally spaced) and explicitly includes the effect of bond breaking.[68] This can be illustrated graphically with Figure 17.

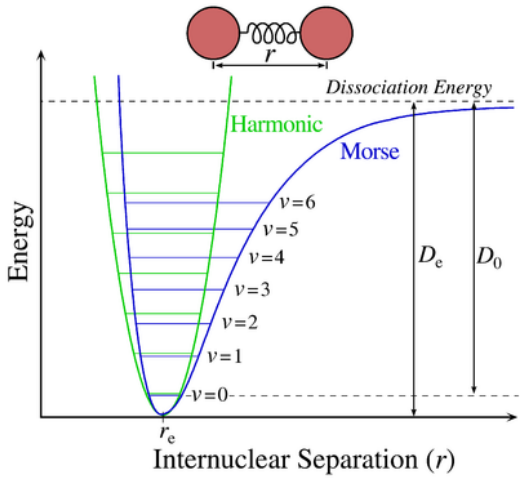

Figure 17. Energy as a function of internuclear separation expressed with Harmonic (green) and Morse (blue) potentials. The Morse potential description of the anharmonicity of the vibrational energy levels show that the spacing decreases as the energy approaches dissociation energy. The zero-point energy of the lowest vibrational level (v = 0) leads to the dissociation energy D_e being greater than the actual energy required for dissociation D_0.[91]

The Morse potential energy function takes the form:

$$V(r) = D_e(1 - e^{-a(r-r_e)})^2 \quad (14)$$

Where r is the internuclear distance; r_e is the equilibrium bond distance, D_e is the well depth; and a determines the width of the potential. While the pair of atoms that are bonded vibrates, its energy fluctuates within the energy dip. However, the atoms will cease to be bonded when the vibrational energy becomes more than the attractive forces between the atoms. At this point, the bond can be considered broken.[22] For this work (specifically, for the definition of a forming event in the computer-based automated method), the chosen internuclear distance at which a bond is considered broken or formed is based on the Van der Waals (VdW) radii of the atoms in question. The van der Waals radius of an atom refers to the radius of a hypothetical

rigid sphere that represents the closest possible approach of another atom to it.[22] For this work, the maximum internuclear distance expected to have a bond was set to be the sum of the Van der Waals radii of the species. Above this point, the bond can be said to have broken; and below this point, a bond can be said to exist. This has been used to define bond breaking in transition structures, making it a good basis upon which bond forming events in the database are established.[68] Table 3 shows reported Van der Waals radii for the three atoms in our system.

Table 3. Van der Waals radii of the three atoms pertinent to methyl linoleate.[92] Initial structure of methyl linoleate have C-C, C-H, and C-O bonds, with maximum internuclear distances for a bond to exist being 3.4 Å, 2.9 Å, and 3.22 Å respectively.

Element	VdW Radius (Å)
Hydrogen	1.20
Carbon	1.70
Oxygen	1.52

CHAPTER 4: RESULTS AND DISCUSSIONS

4.1 AIMD Database Human-Oriented Visual Analysis (HOVA) Results

In describing observations of the visual analysis, there are different angles to use. To describe the results of this research, Figure 18 below serves as a scheme for effective representation of bonds and atoms of the methyl linoleate molecule.

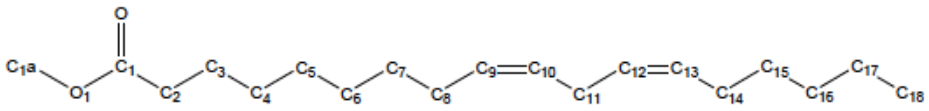

Figure 18. The numbering scheme for methyl linoleate adopted for describing bond cleavages in the simulation.

4.2 Top Level Description of Results

A total of 100 trajectories were observed for bond breaking and forming events. These trajectories were observed using a software called Avogadro.[93] Avogadro is an advanced molecule editor and visualizer, developed by the Avogadro project, specifically designed to be used across different platforms in computational chemistry, bioinformatics, materials science, and other related fields. It can be used to create molecular structures, format input files, and analyze the output of various computational chemistry packages.[93] The trajectories in the AIMD database are opened with Avogadro and played as an animation. This is then watched closely by a human (myself in this case) for times where atoms move too far apart such that corresponding bonds are broken or where atoms move so close that a bond is formed. The bonds, as they break and form, are literally seen in the movie. Figure 19 is a picture of a methyl linoleate trajectory where a bond is observed to have broken. Sometimes, atoms may vibrate such that they go relatively far from each other, and Avogadro displays the bonds between them as temporarily

broken when truly they are not. To reduce the possibility of logging this occurrence as an event, the trajectory is observed for some more time. If atoms remain far apart and do not join back, then it is safe to log the event.

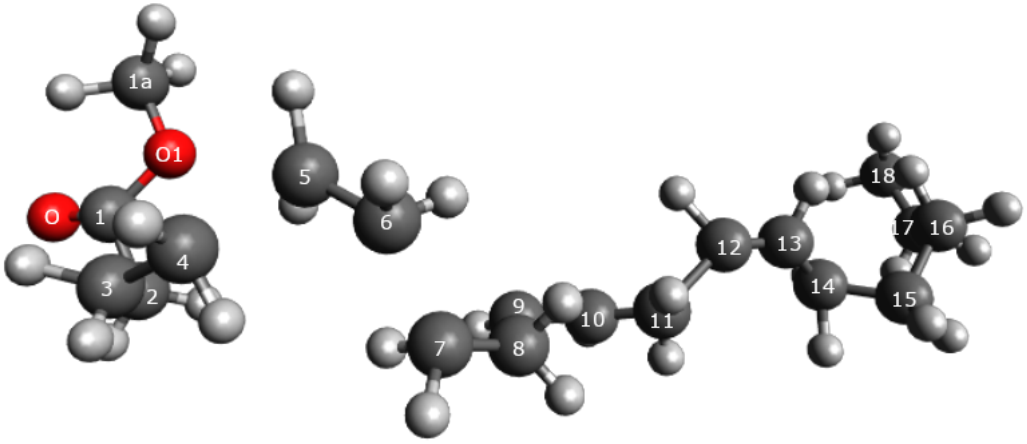

Figure 19. An example trajectory where C_4-C_5 and C_6-C_7 bonds are observed to have broken, producing 1 x C1-C4, 1 x carbonyl, and 1 x C6-C8 products.

To validate this analysis method, theoretical data is compared with experimental data. 68% of the corresponding fatty acid of methyl linoleate, linoleic acid, have been reported to be conserved during thermal decomposition.[22] This, to a good degree, is in alignment with results from our computational simulation where 72% did not dissociate.

Still on validating this method, experimental interpretation of products from linoleic acid pyrolysis have been reported by Asomaning *et. al*. (2014) (earlier reviewed in chapter 1).[58] The gas and liquid product fractions were analyzed and identified using gas chromatography and mass spectrometry, suggesting that solid fractions were negligible. The theoretical results are aligned with this as there is little or no presence of higher weight products than the original molecule. The gas-phase accounted for 15.55 - 30.9 wt. % of the feed, primarily characterized by low weight hydrocarbons (C_1-C_4), CO_2, CO, and H_2. The liquid phase was approximately 68.79 – 87.66 wt. % of the feed, primarily characterized by high weight hydrocarbons (C_6-C_{18}) and

carbonyls.[58] Figure 20 provide the product distribution obtained from the AIMD database and Asomaning *et al*. (2014) study.

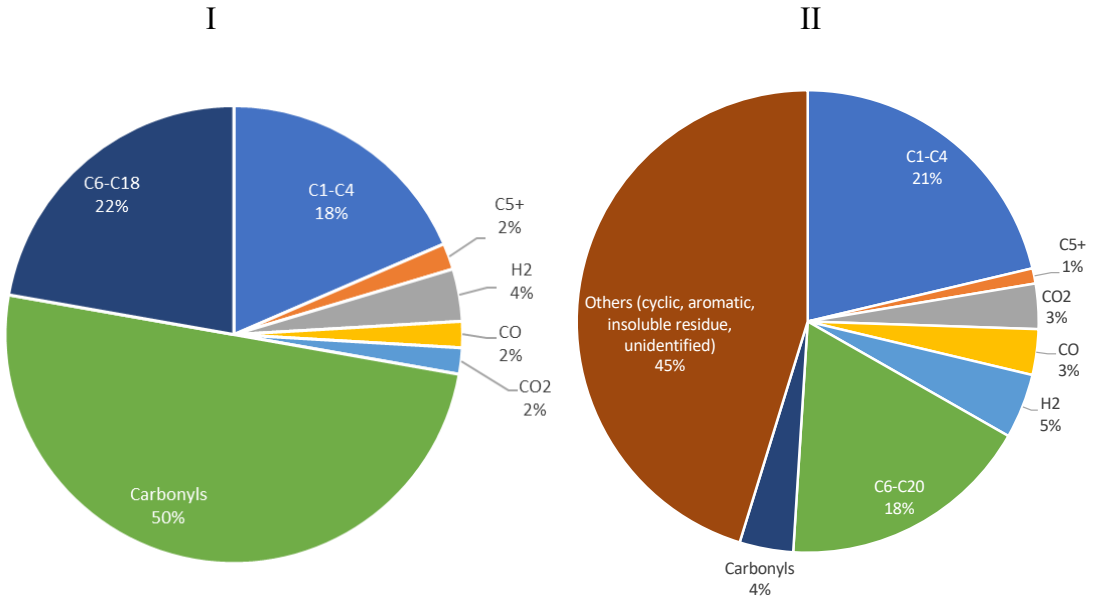

Figure 20. Pyrolysis product distribution obtained from **(I)** AIMD database, and **(II)** Asomaning *et. al.* (2014). Categories are displayed based on categories adopted by Asomaning *et. al*. (2014).[58]

Since the initial state of each trajectory is a molecule with atoms bonded to one another, it is expected that the first events will be bond breaking. A total of 28 trajectories (28%) dissociated, and 72 did not. The maximum number of dissociations (only bond breaking events) per trajectory was 5, and minimum was 1. The average time it took the first breaking event to occur was 416 fs. Figure 21 illustrates the frequency of all bond dissociations.

We observed high frequency of hydrogen abstraction in the methyl moiety of the molecule even though we expect bond dissociation energies for this particular C-H bond to be higher than most C-H bond in the molecule (all with the exception of C-H bonds associated with sp2 hybridized carbons). This observation can be explained by several factors. One of such factors is steric effect which happens because the bulky linoleate moiety easily stabilizes the

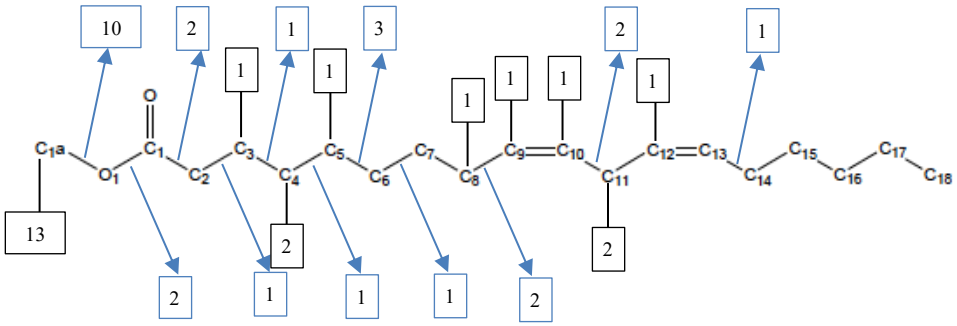

Figure 21. Frequency of total bond dissociations. Black line indicates C-H bond dissociations while blue arrows indicate corresponding C-O and C-C bond dissociations.

resulting radical. Another explanation is the presence of the electronegative atom oxygen. Oxygen's electronegativity results in delocalizing electron density from the radical that is formed upon cleavage, thus stabilizing it. Generally C-H bonds have higher BDEs than C-C.[94] The observations from Figure 21 regarding the frequency of C-H bond scissions align with the general expectation that higher bond dissociation energies (BDEs) correspond to stronger bonds. It is evident that most C-H scissions either do not occur or occur just once. This observation supports the understanding that C-H bonds with higher BDEs are less prone to breaking, indicating their stronger nature. However, two C-H bond dissociations (C_4-H and C_{11}-H) occur more frequently (two times). The reason for this is that C_{11} is a bis-allylic site. A bis-allylic site refers to a specific chemical moiety within a molecule that contains two adjacent allylic groups. An allylic group consists of atoms bonded to a carbon-carbon double bond, which is located next to another carbon-carbon double bond. The BDE for bis-allylic C-H bond is relatively low (< 88kcal/mol).[94] On the other hand, C_4-H scission is a result from C_5-C_6 scission (a significant event, as discussed in the next section). An illustration is given in Figure 22.

The high frequency of the methoxy bond (C_{1a}-H) scission is because of resonance effect from the carbonyl moiety. In the event that this scission occurs, the presence of conjugated

double bonds in the linoleate moiety can lead to resonance stabilization of the resulting linoleate radical.

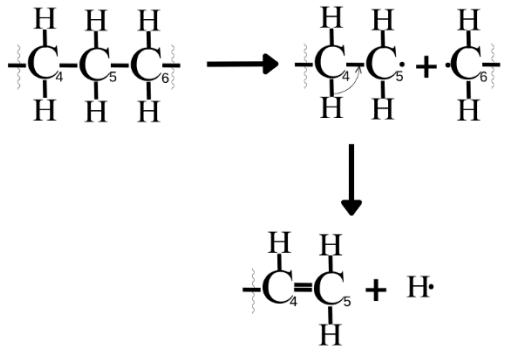

Figure 22. Illustration of C_4-H scission.

The high frequency of the methoxy bond (C_{1a}-H) scission is because of resonance effect from the carbonyl moiety. In the event that this scission occurs, the presence of conjugated double bonds in the linoleate moiety can lead to resonance stabilization of the resulting linoleate radical.

4.3 Granular Level Description of Results

A test for statistical significance was done on the 28 trajectories that dissociated. While these 28 trajectories dissociated, some of the dissociations may be due to random chance. The essence of this statistical test was to eliminate, to a high degree, the possibility of reporting events that happened due to chance. It is important to note that within the 28 trajectories that dissociated, some events occurred more than once, leading to 10 distinct first (breaking) events, only three of which were found to be statistically significant, leading to the conclusion that a larger ensemble is needed to accurately describe the system. Table 4 shows this.

Table 4. Statistical analysis of events. Only three events are significant.

Type	Atom 1	Atom 2	Frequency	$\hat{p}$	C. I.	Sig?
Break	C_{1a}	O_1	9	0.3333	0.1778	Sig
Break	C_{1a}	H	6	0.2222	0.1568	Sig
Break	C_5	C_6	4	0.1481	0.1340	Sig
Break	C_{10}	C_{11}	3	0.1111	0.1185	Not Sig
Break	C_8	C_9	1	0.0370	0.1185	Not Sig
Break	C_1	C_2	1	0.0370	0.1185	Not Sig
Break	C_2	C_3	1	0.0370	0.1185	Not Sig
Break	C_3	C_4	1	0.0370	0.1185	Not Sig
Break	C_4	C_5	1	0.0370	0.1185	Not Sig
Break	C_{13}	C_{14}	1	0.0370	0.1185	Not Sig

4.4 Bond Dissociation Energy (BDE) Analysis

Bond dissociation energies (BDE) have been used in previous studies to assess the energetics and thermochemical properties of a system. Since the primary path of pyrolysis is homolytic bond cleavages, BDE calculations will be vital in describing our system. Bond dissociation energy calculations were performed on first bond breaking events. It is rational to expect that bonds with high BDEs will have low frequency of dissociations. Figure 23 is an illustration of the BDEs of the first 10 distinct events.

In comparison to the study done by Wilson and Siebert, this study considers both kinetic and thermodynamic preferences, including redistribution of vibrational energies. The redistribution of vibrational energy in large chemical compounds happens when energy is exchanged between different vibrational modes within the molecule. Complex molecules, like methyl linoleate, possess multiple vibrational modes associated with distinct molecular motions,

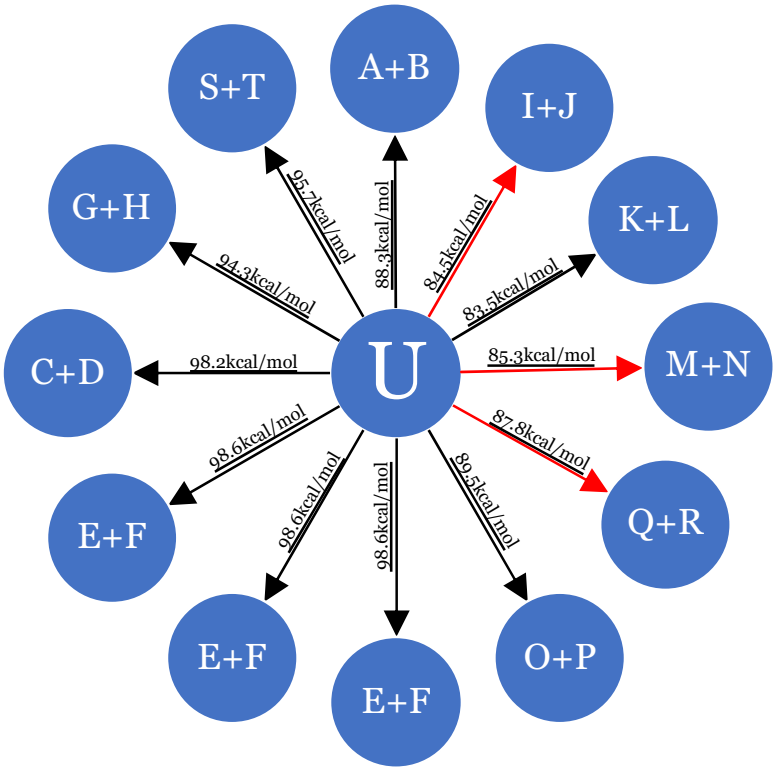

KEYS
(Corresponding bonds in italics)

A+B	=	$C_6H_{11}O_2 + C_{13}H_{23}H$ *(C5-C6)*	M+N	=	$C_5H_9O_2 + C_{14}H_{25}$ *(C4-C5)*
C+D	=	$C_9H_{17}O_2 + C_{10}H_{17}$ *(C8-C9)*	E+F	=	$H + C_{19}H_{33}O_2$ *(Cx-H)*
E+F	=	$H + C_{19}H_{33}O_2$ *(Cx-H)*	O+P	=	$CH_3 + C_{18}H_{31}O_2$ *(Cx-Oa)*
G+H	=	$C_2H_3O_2 + C_{17}H_{31}$ *(C1-C2)*	E+F	=	$H + C_{19}H_{33}O_2$ *(Cx-H)*
I+J	=	$C_3H_5O_2 + C_{16}H_{29}$ *(C2-C3)*	Q+R	=	$C_4H_7O_2 + C_{15}H_{27}$ *(C3-C4)*
K+L	=	$C_{11}H_{19}O_2 + C_8H_{15}$ *(C10-C11)*	S+T	=	$C_{14}H_{23}O_2 + C_5H_{11}$ *(C13-C14)*

Figure 23. BDEs for first (breaking) events. "U" denotes the starting material (methyl linoleate).

such as stretching and bending. When energy is initially introduced into a specific vibrational mode, it can subsequently spread and redistribute across other vibrational modes within the molecule. This energy redistribution process allows the molecule to dynamically transfer and share vibrational energy, impacting its overall vibrational behavior and thermal properties. Table 5 compares BDEs of this study with BDEs of Wilson and Siebert's study. The difference

observed between these studies may be positive or negative and is solely due to conformational differences. Hence, the absolutes are presented.

Table 5. BDE (in kcal/mol) comparison between this study and that of Wilson and Siebert.

Bond	This study	Wilson and Siebert[83]	Absolute difference
C_1-C_2	94.3	95.0	0.7
C_2-C_3	84.5	85.2	0.7
C_3-C_4	87.8	88.6	0.8
C_4-C_5	85.3	88.2	2.9
C_5-C_6	88.3	88.4	0.1
C_8-C_9	98.2	98.7	0.5
C_{10}-C_{11}	88.5	83.4	5.1
C_{13}-C_{14}	95.7	97.6	1.9
C_{1a}-H	98.6	97.8	0.8
C_{1a}-O_a	89.5	91.2	1.7

The difference observed in bond C_{10}-C_{11} is large relative to the others. It is worthy of note that C_{11} is a bis-allylic site and can explain the exception. The vibrational modes associated with the double bonds in the allylic groups can interact with each other, leading to vibrational coupling and energy redistribution. This discrepancy could be explained by redistribution of vibrational energies. When the energy is redistributed away from the bond we want to break, it means that less energy is concentrated in that specific bond. In this case, when we apply additional energy to break the bond, we need to provide more energy because the bond is not weakened by the redistributed vibrational energy. This can increase the apparent BDE because more additional energy is required to break the bond.

The BDE analysis fails to explain possible later dissociations. From Figure 23 and Figure 21, BDE calculations for bonds between C_2 – C_4 (between 84.5kcal/mol and

87.8kcal/mol) are lower than that of $C_1 – C_2$ (94.3kcal/mol), thus we should expect a higher frequency of dissociations from those bonds than $C_1 – C_2$ bond, but this is not the case (as seen in Figure 18). To explain this deviation, later dissociations, or possibly complete dissociations, should be analyzed. In the visual analysis, C_1 - C_2 cleavage occurred only twice: (1) in a trajectory with it as the only event; and (2) in a trajectory with several events but $C_1 – C_2$ cleavage was the last event in the trajectory at time step 766. This trajectory had a total simulation time of 845 fs. Some fragments from trajectory in (2) are C_2H_4 and CHO. These fragments include very stable molecules like H_2 and CO in their structures.[95,96] Since chemical reactions proceed in the most energetically favored path, an explanation for this observation in our database could be that the simulation time may not be long enough to observe further dissociations. In Figure 24, three potential sites for significant bond cleavage are identified based on their relatively low BDEs when compared with BDEs of bonds that cleaved more frequently. Although other factors might be at play here (such as later dissociations discussed above, or smaller Van der Walls radii that defines bond breaking), the magnitude of the difference (14.1 kcal/mol) is too large to ignore. This further reiterates the need for a larger ensemble of trajectories.

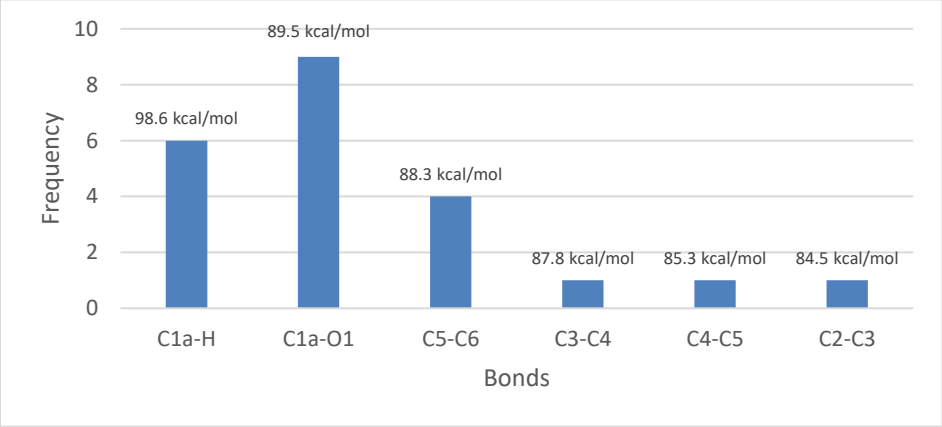

Figure 24. BDEs obtained from significant bond breaking events vs selected bonds with low BDEs being identified as potential sites for significant bond cleavage.

4.5 Assessment of Computer-Based Analysis Method

The development of this method is proving to be very promising. A very significant agreement between the human-oriented visual analysis (HOVA) and the computer-based automated method (CBAM) have been recorded. Table 6 is a confusion matrix that illustrates the alignment of both methods.

Table 6. Confusion matrix illustrating the alignment of the human-oriented visual method and the new computer-based automated method.

	HOVA	
CBAM	Eventful	Non-eventful
Eventful	28	0
Non-eventful	1	71

The confusion matrix is a tabular representation used to assess the effectiveness of the automated method by comparing its output with the results obtained from the visual analysis. It provides a concise summary of the CBAM performance by categorizing the results into true positives (28), false positives (0), true negatives (71), and false negatives (1). The four categories are outlined below:

- True Positive (TP): The method correctly aligned with the HOVA eventful class (number of trajectories that dissociated). CBAM and HOVA both recorded 28 trajectories for this.
- False Positive (FP): The method logged events when HOVA recorded no events. In the above matrix, there are no trajectories in this category.
- True Negative (TN): The method correctly aligned with the HOVA non-eventful class (number of trajectories that did not dissociate). CBAM and HOVA both recorded 71 trajectories for this.

- False Negative (FN): The method did not log events when HOVA recorded events. In the above matrix, there is only one trajectory in this category.

This is a very significant agreement between both methods indicating that development of the CBAM is very promising. Only one out of one hundred trajectories fall out of alignment (99% agreement). However, some anomalies were also recorded. These anomalies will be presented and discussed.

The time logged by the computer for breaking events happened to be significantly far from that of the HOVA. The average difference between the timesteps from both methods is 171.96 fs. As described in the previous chapter, breaking events are defined in the code as a function of the velocities of atoms. Further investigations revealed that velocities kick in much earlier than when the bonds were spotted to be broken in the actual trajectory movie watched with Avogadro, and this is why CBAM logs breaking events earlier than HOVA. An illustration of this is seen in Figure 25.

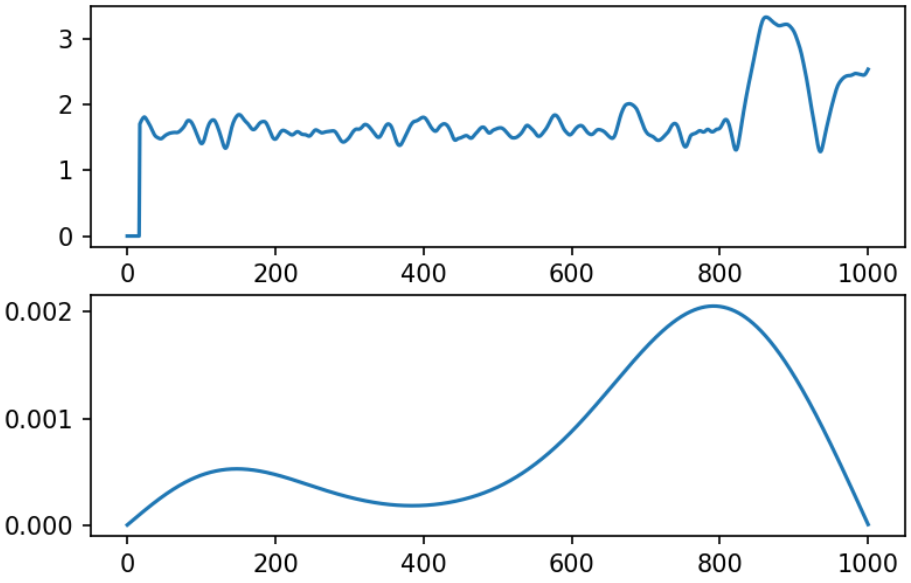

Figure 25. Graphs of interatomic distance (top) and velocity (bottom) vs timestep for the first trajectory (J0001), for atoms C5 and C6. The break threshold velocity is set at 0.002 Å/fs. This break threshold is met at timestep 760 fs as against the timestep where actual cleavage occurs in the visual analysis done with Avogadro (838 fs).

Another anomaly observed was that CBAM fails to log breaking events that occurred close to the end of the trajectory. This is related to the first anomaly in that breaking events are defined by velocities, which are consequently defined by time. Being that the event happens towards the end, there is not sufficient time to compute velocity. Since the root cause of these two issues is in the way that breaking events are being defined, redefinition may be instrumental in solving them. The last anomaly observed was with forming events specifically for H_2 (i.e., H + H). The time logged by the CBAM was significantly far from that of the HOVA. The average difference between the timesteps from both methods is 519.5 fs. The CBAM logs the forming event later than the HOVA. While this is still being investigated, a theory that can explain this observation is based on the fact that the CBAM takes into account the possibility of a rebreak such that the forming event would not be logged if it breaks again within a short time. The atomic mass of the hydrogen atom is considerably smaller relative to carbon and oxygen. The small mass can explain why the hydrogen atom will move with high velocities (farther distances in short times) and any bonds that were formed between them will be broken again. Figure 26 is a plot of the interatomic distances per time step between two hydrogen atoms where this issue is observed.

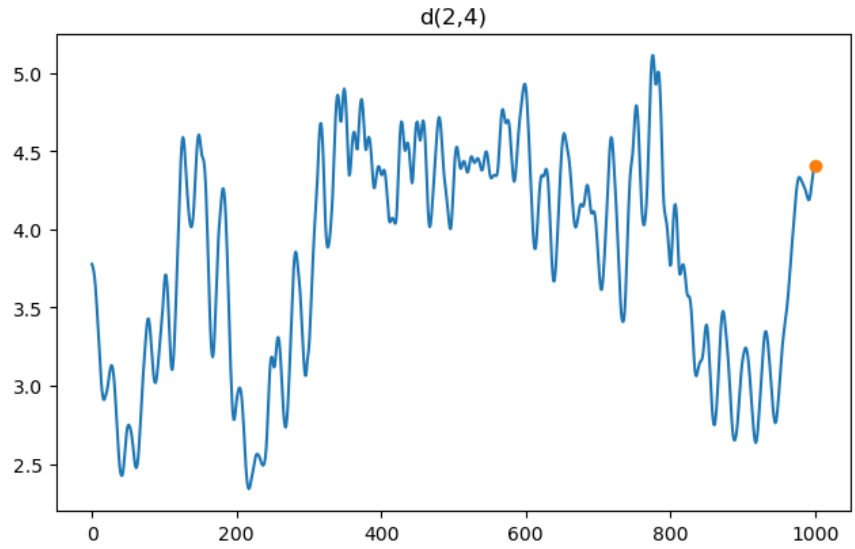

Figure 26. Interatomic distances (d) between two hydrogen atoms (with indices 2 and 4) per time step. These atoms are initially not bonded but later became bonded early in the trajectory. However, CBAM logged the forming event at 841 fs. Before this point, the interatomic distances became high again shortly after the bond formed. Only after this point do we see that the interatomic distance remains small for a longer time (~120 fs), and then it is logged as a forming event.

CHAPTER 5: CONCLUSION AND FUTURE WORK

Thermal decomposition of methyl linoleate was simulated using M06-2X/6-31+G(d,p). The pyrolysis was modeled using AIMD at 3500 K for a suitable time period. By utilizing an *ab initio* approach, we expect a more precise and comprehensive depiction of the pyrolysis process as it provides an atomic-level representation of the FAME system as it progresses in time. Theoretical results were in agreement with experimental data in terms of product distribution. However, BDE analysis revealed that results can be improved by increasing the size of the ensemble and extending the timespan of the trajectory beyond 1000 fs. With the need to create and analyze larger ensembles, there is a need to develop an automated method to improve time effectiveness of the post-simulation analysis and reduce the possibility of human errors. A computer-based automated method is currently being developed and actively being tested and optimized. This automated method has shown significant alignment with data acquired from the human-oriented visual analysis, indicating that the automated method works well and can be improved to meet required standards. However, some anommalies were observed in the results from the automated method. All three anomalies are linked to how the events are determined and logged by the method, two of which are in the breaking category and the last one is in the forming category (specifically between two hydrogen atoms). Finding another way to redefine these events in the method is a potential solution to these problems.

This research is still ongoing, but future work would include AIMD investigations with this method on other FAMEs (methyl palmitate, methyl linolenate, methyl stearate, etc). Recommendations such as using larger ensembles with trajectories that have longer simulation time may be adopted for these future investigations. However, it is important to note that it takes

a considerable amount of time to produce a single trajectory (~72 hours for this work) and increasing the simulation time may increase the production time, making the research more computationally expensive. Thus, it is recommended that higher computational infrastructure be used for future investigations. This is important as such investigations will provide grounds for understanding the influence of molecular structure on the pyrolysis path. This understanding is crucial in determining and designing ideal FAMEs that would dissociate to produce useful industrial compounds. Investigations can also be done with triglycerides, the feed that produces biodiesel. Furthermore, the automated method should continue to be finetuned to meet required standards. This will definitely be a breakthrough in the computational chemistry space.

REFERENCES

(1) Eneh, O. C. A Review on Petroleum: Source, Uses, Processing, Products and the Environment. *J. of Applied Sciences* **2011**, *11* (12), 2084–2091. https://doi.org/10.3923/jas.2011.2084.2091.

(2) Huang, D.; Zhou, H.; Lin, L. Biodiesel: An Alternative to Conventional Fuel. *Energy Procedia* **2012**, *16*, 1874–1885. https://doi.org/10.1016/j.egypro.2012.01.287.

(3) Hussain, N. *Composition of Crude Oil The Petro Solutions*. The Petro Solutions. https://thepetrosolutions.com/composition-of-crude-oil/ (accessed 2023-03-15).

(4) Humans, I. W. G. on the E. of C. R. to. *CRUDE OIL*; International Agency for Research on Cancer, **1989**.

(5) *Refining crude oil - U.S. Energy Information Administration (EIA)*. https://www.eia.gov/energyexplained/oil-and-petroleum-products/refining-crude-oil.php (accessed 2023-03-15).

(6) Speight, J. G. Chapter 3 - Hydrocarbons from Crude Oil. In *Handbook of Industrial Hydrocarbon Processes (Second Edition)*; Speight, J. G., Ed.; Gulf Professional Publishing: Boston, **2020**; pp 95–142. https://doi.org/10.1016/B978-0-12-809923-0.00003-5.

(7) Boulamanti, A.; Moya, J. A. Production Costs of the Chemical Industry in the EU and Other Countries: Ammonia, Methanol and Light Olefins. *Renewable and Sustainable Energy Reviews* **2017**, *68*, 1205–1212. https://doi.org/10.1016/j.rser.2016.02.021.

(8) Gourmelon, G. Global Plastic Production Rises, Recycling Lags, 2015. chrome-extension://efaidnbmnnnibpcajpcglclefindmkaj/http://www.plastic-resource-center.com/wp-content/uploads/2018/11/Global-Plastic-Production-RisesRecycling-Lags.pdf (accessed 2023-03-15).

(9) *Reproductive Effects of Oil-Related Environmental Pollutants - ScienceDirect*. https://www.sciencedirect.com/science/article/pii/B9780124095489110395 (accessed 2023-03-18).

(10) Katz, D. L.; Beu, K. E. Nature of Asphaltic Substances. *Ind. Eng. Chem.* **1945**, *37* (2), 195–200. https://doi.org/10.1021/ie50422a022.

(11) *Refining crude oil - inputs and outputs - U.S. Energy Information Administration (EIA)*. https://www.eia.gov/energyexplained/oil-and-petroleum-products/refining-crude-oil-inputs-and-outputs.php (accessed 2023-02-15).

(12) *Years of fossil fuel reserves left*. Our World in Data. https://ourworldindata.org/grapher/years-of-fossil-fuel-reserves-left (accessed 2023-03-18).

(13) Ritchie, H.; Roser, M.; Rosado, P. Energy. *Our World in Data* **2022**.

(14) Agarwal, A. K. Biofuels (Alcohols and Biodiesel) Applications as Fuels for Internal Combustion Engines. *Progress in Energy and Combustion Science* **2007**, *33* (3), 233–271. https://doi.org/10.1016/j.pecs.2006.08.003.

(15) Wu, D.; Zhang, F.; Lou, W.; Li, D.; Chen, J. Chemical Characterization and Toxicity Assessment of Fine Particulate Matters Emitted from the Combustion of Petrol and Diesel Fuels. *Science of The Total Environment* **2017**, *605–606*, 172–179. https://doi.org/10.1016/j.scitotenv.2017.06.058.

(16) Thuiller, W. Climate Change and the Ecologist. *Nature* **2007**, *448* (7153), 550–552. https://doi.org/10.1038/448550a.

(17) Worley, J. Greenhouses: Heating, Cooling and Ventilation.
(18) *FAQ 1.3 - AR4 WGI Chapter 1: Historical Overview of Climate Change Science*. https://archive.ipcc.ch/publications_and_data/ar4/wg1/en/faq-1-3.html (accessed 2023-07-13).
(19) US EPA, O. *Overview of Greenhouse Gases*. https://www.epa.gov/ghgemissions/overview-greenhouse-gases (accessed 2023-03-21).
(20) Lashof, D. A.; Ahuja, D. R. Relative Contributions of Greenhouse Gas Emissions to Global Warming. *Nature* **1990**, *344* (6266), 529–531. https://doi.org/10.1038/344529a0.
(21) US EPA, O. *Effects of Acid Rain*. https://www.epa.gov/acidrain/effects-acid-rain (accessed 2023-03-20).
(22) Bakker, M. Improving Biodiesel Through Pyrolysis: Direct Dynamics Investigations into Thermal Decomposition of Methyl Linoleate. *MSU Graduate Theses* **2020**.
(23) Roser, M.; Ritchie, H. Oil Spills. *Our World in Data* **2022**.
(24) *Oil and the environment - U.S. Energy Information Administration (EIA)*. https://www.eia.gov/energyexplained/oil-and-petroleum-products/oil-and-the-environment.php (accessed 2023-03-22).
(25) *U.S. Regulation of Oil and Gas Operations*. American Geosciences Institute. https://www.americangeosciences.org/geoscience-currents/us-regulation-oil-and-gas-operations (accessed 2023-03-21).
(26) Lujala, P. Deadly Combat over Natural Resources: Gems, Petroleum, Drugs, and the Severity of Armed Civil Conflict. *The Journal of Conflict Resolution* **2009**, *53* (1), 50–71.
(27) Pineda, M. E. *Why Are Oil and Gas Prices Going Up: Impact of Russia-Ukraine War*. Profolus. https://www.profolus.com/topics/why-are-oil-and-gas-prices-going-up-impact-of-russia-ukraine-war/ (accessed 2023-03-25).
(28) *How does the war in Ukraine affect oil prices?*. World Economic Forum. https://www.weforum.org/agenda/2022/03/how-does-the-war-in-ukraine-affect-oil-prices/ (accessed 2023-03-25).
(29) Mohammed, N. The Russia-Ukraine War Crisis - It's Impact on Indian Economy. Rochester, NY April 10, **2022**. https://papers.ssrn.com/abstract=4080234 (accessed 2023-03-25).
(30) Herzog, A. V.; Lipman, T. E.; Kammen. Renewable Energy Sources. *Encyclopedia of Life Support Systems (EOLSS)* **2001**, *Forerunner Volume-'Perspectives and Overview of Life Support Systems and Sustainable Development' 76*.
(31) Wang, S.; Wang, S. Impacts of Wind Energy on Environment: A Review. *Renewable and Sustainable Energy Reviews* **2015**, *49*, 437–443. https://doi.org/10.1016/j.rser.2015.04.137.
(32) Lakatos, L.; Hevessy, G.; Kovács, J. Advantages and Disadvantages of Solar Energy and Wind-Power Utilization. *World Futures* **2011**, *67* (6), 395–408. https://doi.org/10.1080/02604020903021776.
(33) Askari, M.; Mirzaei Mahmoud Abadi, V.; Mirhabibi, M.; Dehghani, P. Hydroelectric Energy Advantages and Disadvantages. *American Journal of Energy Science* **2015**, *2*, 17–20.
(34) Fearnside, P. M. Do Hydroelectric Dams Mitigate Global Warming? The Case of Brazil's CuruÁ-Una Dam. *Mitig Adapt Strat Glob Change* **2005**, *10* (4), 675–691. https://doi.org/10.1007/s11027-005-7303-7.

(35) Bloomquist, G.; Lund, J.; Gehringer, M. Geothermal Energy. In *The World Scientific Handbook of Energy*; Materials and Energy; WORLD SCIENTIFIC, **2012**; Vol. Volume 3, pp 245–273. https://doi.org/10.1142/9789814343527_0012.
(36) Field, C. B.; Campbell, J. E.; Lobell, D. B. Biomass Energy: The Scale of the Potential Resource. *Trends in Ecology & Evolution* **2008**, *23* (2), 65–72. https://doi.org/10.1016/j.tree.2007.12.001.
(37) Hall, D. O. Biomass Energy. *Energy Policy* **1991**, *19* (8), 711–737. https://doi.org/10.1016/0301-4215(91)90042-M.
(38) Tursi, A. A Review on Biomass: Importance, Chemistry, Classification, and Conversion. *Biofuel Research Journal* **2019**, *6*, 962–979. https://doi.org/10.18331/BRJ2019.6.2.3.
(39) Ma, F.; Hanna, M. A. Biodiesel Production: A Review1Journal Series #12109, Agricultural Research Division, Institute of Agriculture and Natural Resources, University of Nebraska–Lincoln.1. *Bioresource Technology* **1999**, *70* (1), 1–15. https://doi.org/10.1016/S0960-8524(99)00025-5.
(40) Vasudevan, P. T.; Briggs, M. Biodiesel Production—Current State of the Art and Challenges. *Journal of Industrial Microbiology and Biotechnology* **2008**, *35* (5), 421. https://doi.org/10.1007/s10295-008-0312-2.
(41) Abbaszaadeh, A.; Ghobadian, B.; Omidkhah, M. R.; Najafi, G. Current Biodiesel Production Technologies: A Comparative Review. *Energy Conversion and Management* **2012**, *63*, 138–148. https://doi.org/10.1016/j.enconman.2012.02.027.
(42) *9.2 The Reaction of Biodiesel: Transesterification | EGEE 439: Alternative Fuels from Biomass Sources*. https://www.e-education.psu.edu/egee439/node/684 (accessed 2022-07-14).
(43) Kubátová, A.; Šťávová, J.; Seames, W. S.; Luo, Y.; Sadrameli, S. M.; Linnen, M. J.; Baglayeva, G. V.; Smoliakova, I. P.; Kozliak, E. I. Triacylglyceride Thermal Cracking: Pathways to Cyclic Hydrocarbons. *Energy Fuels* **2012**, *26* (1), 672–685. https://doi.org/10.1021/ef200953d.
(44) *Monthly Biodiesel Production Report - Energy Information Administration*. https://www.eia.gov/biofuels/biodiesel/production/ (accessed 2023-04-21).
(45) *Biofuels and the environment - U.S. Energy Information Administration (EIA)*. https://www.eia.gov/energyexplained/biofuels/biofuels-and-the-environment.php (accessed 2023-04-21).
(46) *Alternative Fuels Data Center: Biodiesel Benefits*. https://afdc.energy.gov/fuels/biodiesel_benefits.html (accessed 2023-04-21).
(47) Fargione, J.; Hill, J.; Tilman, D.; Polasky, S.; Hawthorne, P. Land Clearing and the Biofuel Carbon Debt. *Science* **2008**, *319* (5867), 1235–1238. https://doi.org/10.1126/science.1152747.
(48) Gerbens-Leenes, W.; Hoekstra, A. Y.; van der Meer, T. H. The Water Footprint of Bioenergy. *Proceedings of the National Academy of Sciences* **2009**, *106* (25), 10219–10223. https://doi.org/10.1073/pnas.0812619106.
(49) Crutzen, P. J.; Mosier, A. R.; Smith, K. A.; Winiwarter, W. N2O Release from Agro-Biofuel Production Negates Global Warming Reduction by Replacing Fossil Fuels. In *Paul J. Crutzen: A Pioneer on Atmospheric Chemistry and Climate Change in the Anthropocene*; Crutzen, P. J., Brauch, H. G., Eds.; SpringerBriefs on Pioneers in Science and Practice; Springer International Publishing: Cham, **2016**; pp 227–238. https://doi.org/10.1007/978-3-319-27460-7_12.

(50) Demirbas, A. Progress and Recent Trends in Biodiesel Fuels. *Energy Conversion and Management* **2009**, *50* (1), 14–34. https://doi.org/10.1016/j.enconman.2008.09.001.
(51) You, Y.-D.; Shie, J.-L.; Chang, C.-Y.; Huang, S.-H.; Pai, C.-Y.; Yu, Y.-H.; Chang, C. H. Economic Cost Analysis of Biodiesel Production: Case in Soybean Oil. *Energy Fuels* **2008**, *22* (1), 182–189. https://doi.org/10.1021/ef700295c.
(52) Dunn, R. O. Effect of Antioxidants on the Oxidative Stability of Methyl Soyate (Biodiesel). *Fuel Processing Technology* **2005**, *86* (10), 1071–1085. https://doi.org/10.1016/j.fuproc.2004.11.003.
(53) Pérez, Á.; Casas, A.; Fernández, C. M.; Ramos, M. J.; Rodríguez, L. Winterization of Peanut Biodiesel to Improve the Cold Flow Properties. *Bioresource Technology* **2010**, *101* (19), 7375–7381. https://doi.org/10.1016/j.biortech.2010.04.063.
(54) Nnaemeka, O. J.; Bibeau, E. L. Application of Low-Temperature Phase Change Materials to Enable the Cold Weather Operability of B100 Biodiesel in Diesel Trucks. *Journal of Energy Resources Technology* **2019**, *141* (6). https://doi.org/10.1115/1.4042409.
(55) Asakuma, Y.; Maeda, K.; Kuramochi, H.; Fukui, K. Theoretical Study of the Transesterification of Triglycerides to Biodiesel Fuel. *Fuel* **2009**, *88* (5), 786–791. https://doi.org/10.1016/j.fuel.2008.10.045.
(56) Bridgwater, A. V. Review of Fast Pyrolysis of Biomass and Product Upgrading. *Biomass and Bioenergy* **2012**, *38*, 68–94. https://doi.org/10.1016/j.biombioe.2011.01.048.
(57) *Potential of pyrolysis processes in the waste management sector - ScienceDirect*. https://www.sciencedirect.com/science/article/pii/S2451904917300690 (accessed 2023-07-07).
(58) Asomaning, J.; Mussone, P.; Bressler, D. C. Pyrolysis of Polyunsaturated Fatty Acids. *Fuel Processing Technology* **2014**, *120*, 89–95. https://doi.org/10.1016/j.fuproc.2013.12.007.
(59) Lappas, A. A.; Bezergianni, S.; Vasalos, I. A. Production of Biofuels via Co-Processing in Conventional Refining Processes. *Catalysis Today* **2009**, *145* (1), 55–62. https://doi.org/10.1016/j.cattod.2008.07.001.
(60) Maher, K. D.; Bressler, D. C. Pyrolysis of Triglyceride Materials for the Production of Renewable Fuels and Chemicals. *Bioresource Technology* **2007**, *98* (12), 2351–2368. https://doi.org/10.1016/j.biortech.2006.10.025.
(61) Adebanjo, A. O.; Dalai, A. K.; Bakhshi, N. N. Production of Diesel-Like Fuel and Other Value-Added Chemicals from Pyrolysis of Animal Fat. *Energy Fuels* **2005**, *19* (4), 1735–1741. https://doi.org/10.1021/ef040091b.
(62) *Glossary - U.S. Energy Information Administration (EIA)*. https://www.eia.gov/tools/glossary/index.php (accessed 2023-07-07).
(63) Rapaport, D. C.; Rapaport, R., Dennis C. *The Art of Molecular Dynamics Simulation*; Cambridge University Press, **2004**.
(64) Allen, M. Introduction to Molecular Dynamics Simulation. *Computational Soft Matter: From Synthetic Polymers to Proteins, Lecture Notes* **2004**, *23*, 1–28.
(65) Cramer, C. J. *Essentials of Computational Chemistry: Theories and Models*; John Wiley & Sons, **2013**.
(66) *Computational Soft Matter: From Synthetic Polymers to Proteins. Lect: Lecture Notes*; NIC series; NIC: Jülich, **2004**.
(67) Lewars, E. G. *Computational Chemistry*; Springer Netherlands: Dordrecht, **2011**. https://doi.org/10.1007/978-90-481-3862-3.

(68) Young, D. *Computational Chemistry: A Practical Guide for Applying Techniques to Real World Problems*; Wiley, **2004**.
(69) Li, H. Conformations of Amino Acids Characterized by Theoretical Spectroscopy, 2014.
(70) Eisberg, R. M.; Resnick, R. *Quantum Physics of Atoms, Molecules, Solids, Nuclei, and Particles*; New York : Wiley, **1985**.
(71) Iftimie, R.; Minary, P.; Tuckerman, M. E. Ab Initio Molecular Dynamics: Concepts, Recent Developments, and Future Trends. *Proceedings of the National Academy of Sciences* **2005**, *102* (19), 6654–6659. https://doi.org/10.1073/pnas.0500193102.
(72) Wilson, Z. Ab Initio Methyl Linoleate Bond Dissociation Energies: First Principles Fishing for Wise Crack Products. *MSU Graduate Theses* **2017**.
(73) Leimkuhler, B.; Matthews, C. *Molecular Dynamics: With Deterministic and Stochastic Numerical Methods*; Interdisciplinary Applied Mathematics; Springer International Publishing: Cham, **2015**; Vol. 39. https://doi.org/10.1007/978-3-319-16375-8.
(74) Xie, Q.; Tinker, R. Molecular Dynamics Simulations of Chemical Reactions for Use in Education. *J. Chem. Educ.* **2006**, *83* (1), 77. https://doi.org/10.1021/ed083p77.
(75) *Modern Methods and Algorithms of Quantum Chemistry. Proc: Proceedings*; NIC series; NIC: Jülich, **2000**.
(76) Admin. *Comprehensive Review of Exchange-Correlation Functional Methods*. NHSJS. https://nhsjs.com/2017/comprehensive-review-of-exchange-correlation-functional-methods/ (accessed 2023-05-02).
(77) Kohn, W.; Sham, L. J. Self-Consistent Equations Including Exchange and Correlation Effects. *Physical Review* **1965**, *140*, 1133–1138. https://doi.org/10.1103/PhysRev.140.A1133.
(78) Perdew, J. P.; Chevary, J. A.; Vosko, S. H.; Jackson, K. A.; Pederson, M. R.; Singh, D. J.; Fiolhais, C. Atoms, Molecules, Solids, and Surfaces: Applications of the Generalized Gradient Approximation for Exchange and Correlation. *Phys. Rev. B* **1992**, *46* (11), 6671–6687. https://doi.org/10.1103/PhysRevB.46.6671.
(79) Zhao, Y.; Truhlar, D. G. Density Functional for Spectroscopy: No Long-Range Self-Interaction Error, Good Performance for Rydberg and Charge-Transfer States, and Better Performance on Average than B3LYP for Ground States. *J. Phys. Chem. A* **2006**, *110* (49), 13126–13130. https://doi.org/10.1021/jp066479k.
(80) Lundberg, M.; Siegbahn, P. E. M. Quantifying the Effects of the Self-Interaction Error in DFT: When Do the Delocalized States Appear? *The Journal of Chemical Physics* **2005**, *122* (22), 224103. https://doi.org/10.1063/1.1926277.
(81) Cohen, A. J.; Mori-Sánchez, P.; Yang, W. Insights into Current Limitations of Density Functional Theory. *Science* **2008**, *321* (5890), 792–794. https://doi.org/10.1126/science.1158722.
(82) Tsuneda, T. *Density Functional Theory in Quantum Chemistry*; Springer Japan: Tokyo, **2014**. https://doi.org/10.1007/978-4-431-54825-6.
(83) Wilson, Z. R.; Siebert, M. R. Methyl Linoleate and Methyl Oleate Bond Dissociation Energies: Electronic Structure Fishing for Wise Crack Products. *Energy Fuels* **2018**, *32* (2), 1779–1787. https://doi.org/10.1021/acs.energyfuels.7b02798.
(84) Zhao, Y.; Truhlar, D. G. The M06 Suite of Density Functionals for Main Group Thermochemistry, Thermochemical Kinetics, Noncovalent Interactions, Excited States, and Transition Elements: Two New Functionals and Systematic Testing of Four M06-Class

Functionals and 12 Other Functionals. *Theor Chem Account* **2008**, *120* (1), 215–241. https://doi.org/10.1007/s00214-007-0310-x.
(85) Mardirossian, N.; Head-Gordon, M. Thirty Years of Density Functional Theory in Computational Chemistry: An Overview and Extensive Assessment of 200 Density Functionals. *Molecular Physics* **2017**, *115* (19), 2315–2372. https://doi.org/10.1080/00268976.2017.1333644.
(86) Sherrill, C. D. Basis Sets in Quantum Chemistry. *School of Chemistry and Biochemistry, Georgia Institute of Technology* **2017**.
(87) *How to Calculate Statistical Significance*. CloudResearch. https://www.cloudresearch.com/resources/guides/statistical-significance/calculate-statistical-significance/ (accessed 2023-02-26).
(88) *Market Anomaly and Arbitrage Opportunity Around Ex-Dividend Day (Management Project) | ProjectAbstracts.com – Projects Ideas and Downloads*. https://projectabstracts.com/17704/market-anomaly-and-arbitrage-opportunity-around-ex-dividend-day.html (accessed 2022-12-04).
(89) Frisch, M. J.; Trucks, G. W.; Schlegel, H. B.; Scuseria, G. E.; Robb, M. A.; Cheeseman, J. R.; Scalmani, G.; Barone, V.; Mennucci, B.; Petersson, G. A.; Nakatsuji, H.; Caricato, M.; Li, X.; Hratchian, H. P.; Izmaylov, A. F.; Bloino, J.; Zheng, G.; Sonnenberg, J. L.; Hada, M.; Ehara, M.; Toyota, K.; Fukuda, R.; Hasegawa, J.; Ishida, M.; Nakajima, T.; Honda, Y.; Kitao, O.; Nakai, H.; Vreven, T.; Montgomery, J. A., Jr.; Peralta, J. E.; Ogliaro, F. O.; Bearpark, M. J.; Heyd, J.; Brothers, E. N.; Kudin, K. N.; Staroverov, V. N.; Kobayashi, R.; Normand, J.; Raghavachari, K.; Rendell, A. P.; Burant, J. C.; Iyengar, S. S.; Tomasi J.; Cossi, M.; Rega, N.; Millam, N. J.; Klene, M.; Knox, J. E.; Cross, J. B.; Bakken, V.; Adamo, C.; Jaramillo, J.; Gomperts, R.; Stratmann, R. E.; Yazyev, O.; Austin, A. J.; Cammi, R.; Pomelli, C.; Ochterski, J. W.; Martin, R. L.; Morokuma, K.; Zakrzewski, V. G.; Voth, G. A.; Salvador, P.; Dannenberg, J. J.; Dapprich, S.; Daniels, A. D.; Farkas, Ã. D. N.; Foresman, J. B.; Ortiz, J. V.; Cioslowski, J.; Fox, D. J. Gaussian 09, Revision D.01, **2009**.
(90) Girod, M.; Grammaticos, B. The Zero-Point Energy Correction and Its Effect on Nuclear Dynamics. *Nuclear Physics A* **1979**, *330* (1), 40–52. https://doi.org/10.1016/0375-9474(79)90535-9.
(91) Morse Potential. *Wikipedia*; **2023**.
(92) Bondi, A. Van Der Waals Volumes and Radii. *J. Phys. Chem.* **1964**, *68* (3), 441–451. https://doi.org/10.1021/j100785a001.
(93) Hanwell, M. D.; Curtis, D. E.; Lonie, D. C.; Vandermeersch, T.; Zurek, E.; Hutchison, G. R. Avogadro: An Advanced Semantic Chemical Editor, Visualization, and Analysis Platform. *Journal of Cheminformatics* **2012**, *4* (1), 17. https://doi.org/10.1186/1758-2946-4-17.
(94) Blanksby, S. J.; Ellison, G. B. Bond Dissociation Energies of Organic Molecules. *Acc. Chem. Res.* **2003**, *36* (4), 255–263. https://doi.org/10.1021/ar020230d.
(95) *2.3b: MO theory of bonding in H_2^+*. Chemistry LibreTexts. https://chem.libretexts.org/Bookshelves/Inorganic_Chemistry/Map%3A_Inorganic_Chemistry_(Housecroft)/02%3A_Basic_Concepts-_Molecules/2.03%3A_Homonuclear_Diatomic_Molecules_-_Molecular_Orbital_(MO)_Theory/2.3b%3A_MO_theory_of_bonding_in_H (accessed 2023-02-25).

(96) Donald, J. A. Subchapter 103B - Carbon Monoxide. In *Handbook of Hormones*; Takei, Y., Ando, H., Tsutsui, K., Eds.; Academic Press: San Diego, **2016**; pp 606-e103B-3. https://doi.org/10.1016/B978-0-12-801028-0.00252-X.